Marine Pollution Bulletin 172 (2021) 112908

Contents lists available at ScienceDirect

Marine Pollution Bulletin

journal homepage: www.elsevier.com/locate/marpolbul

The role of algal blooms and community respiration in controlling the temporal and spatial dynamics of hypoxia and acidification in eutrophic estuaries

Ryan B. Wallace [a,b], Christopher J. Gobler [b,*]

[a] Department of Environmental Studies and Sciences, Adelphi University, Garden City, NY 11530, United States of America
[b] School of Marine and Atmospheric Sciences, Stony Brook University, Southampton, NY 11968, United States of America

ARTICLE INFO

Keywords:
Anthropogenic eutrophication
Acidification
Hypoxia
Respiration
Carbon dioxide
pH
Dissolved oxygen
Ecosystem metabolism

ABSTRACT

While hypoxia and acidification can be common occurrences in eutrophic coastal zones, the precise, coupled temporal and spatial dynamics of these conditions are poorly described. Here, continuous measurements of water column pH, pCO_2, carbonate chemistry, and dissolved oxygen (DO) concentrations were made from spring through fall across two, temperate eutrophic estuaries, western Long Island Sound (LIS) and Jamaica Bay, NY, USA. Vertical dynamics were resolved using an underway towing profiler and an automated stationary profiling unit. During the study, high rates of respiration in surface and bottom waters (> -0.2 mg O_2 L^{-1} h^{-1}) yielded strongly negative rates of net ecosystem metabolism during the summer (-4 to -8 g O_2 m^{-2} d^{-1}). Ephemeral surface algal blooms caused brief periods (< one week) of basification and supersaturation of DO that were succeeded by longer periods of acidification and hypoxia. In deeper regions, hypoxia (< 2 mg L^{-1} DO) and acidic water (pH < 7; total scale; pCO_2 levels >2000 μatm) that persisted continuously for >40 days in both estuaries was often overlain by water with higher DO and pH. Diurnal vertical profiles demonstrated that oxic surface waters saturated with respect to calcium carbonate and DO during the day transitioned to unsaturated and hypoxic at night. Evidence is presented that, beyond respiration, nitrification in surface water promoted by sewage discharge and oxidation processes in sediments also contribute to acidification in these estuaries. Collectively, this study demonstrates the pervasive, persistent, and dynamic nature of hypoxia and acidification in eutrophic estuaries are likely to shape marine food webs.

1. Introduction

During the past decade, coupled hypoxia-acidification has been documented in coastal systems around the globe (Feely et al., 2010; Cai et al., 2011; Wallace et al., 2021). While lower oxygen and pH conditions in ocean surface waters can be a consequence of climate change, highly similar changes can be induced by diverse and dynamic processes within coastal zones (Kelly et al., 2011). Upwelling is a common oceanographic feature present along the west coasts of North America, South America, and Africa and, in recent years, the ability of upwelling in the Pacific Northwest to bring acidic and hypoxic waters into coastal systems has been well-described (Connolly et al., 2010; Roegner et al., 2011; Feely et al., 2018). Such upwelling induced acidification has been cited as the cause of significantly reduced production of wild and aquacultured Pacific oysters (Barton et al., 2012) whose early life stages are highly sensitive to low pH (Waldbusser et al., 2013).

In contrast to western boundary upwelling, hypoxic and acidified conditions in other regions have been often linked to excessive anthropogenic nutrient loading. For example, on the US Gulf Coast agricultural runoff from the Mississippi River can cause intense biological production in surface waters during and after peak river flow in the spring (Turner and Rabalais, 2003; Turner et al., 2003) that promotes hypoxia and acidification in near bottom waters as the Gulf of Mexico stratifies and organic matter from spring production sinks and is remineralized (Cai et al., 2011; Feely et al., 2018). Other coastal zones experience intense nutrient loading and hypoxia as a result of expansive urbanization and associated enhanced wastewater or agricultural flows coupled with restricted ocean exchange (Codiga et al., 2009; Fribance et al., 2013; Wallace and Gobler, 2015). The degradation of organic matter directly and indirectly (enhanced organic matter from primary

* Corresponding author at: School of Marine and Atmospheric Sciences, Stony Brook University, Southampton, NY 11968, United States of America.
E-mail addresses: rwallace@adelphi.edu (R.B. Wallace), christopher.gobler@stonybrook.edu (C.J. Gobler).

https://doi.org/10.1016/j.marpolbul.2021.112908
Received 3 August 2021; Accepted 23 August 2021
Available online 9 September 2021

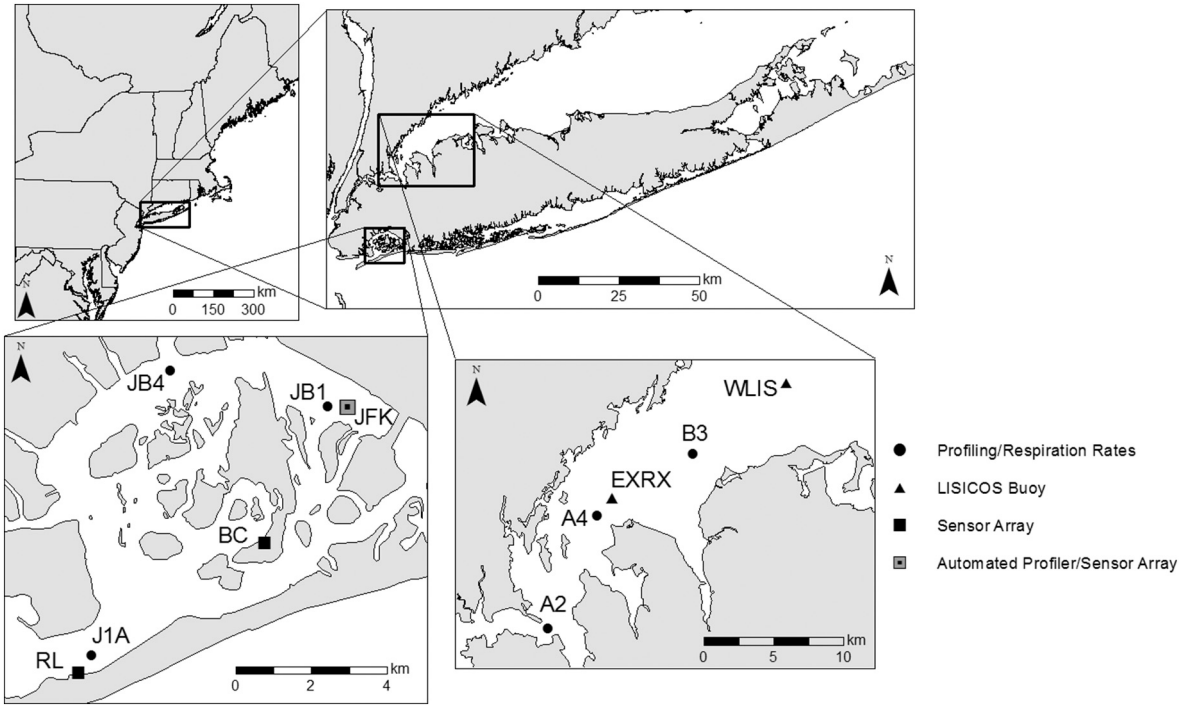

Fig. 1. Top left: Northeast region of the United States and **top right:** Long Island, New York. **Bottom left:** Jamaica Bay and **bottom right:** western Long Island Sound. Black circles indicate diurnal profiling locations and sampling stations in which respiration rates were measured in both Jamaica Bay and Long Island Sound. Black triangles indicate locations in which SeaFET ocean pH sensors were mounted to existing University of Connecticut LISICOS (Long Island Sound Integrated Coastal Observing System) buoys. Black squares indicate Jamaica Bay sensor array and black square surrounded by gray square indicates sensor array station and automated telemetered profiler station. In Jamaica Bay, stations RL and J1A lie within the Rockaway Inlet, station JB4 is in North Channel, station BC is within the central Broad Channel region, and stations JB1 and JFK lie within the Grassy Bay.

producers via nutrient discharge) emanating from wastewater and biological respiration of that organic matter may also create acidified conditions (Wallace et al., 2014; Rheuban et al., 2019). In many eutrophic coastal systems, bottom water hypoxia and acidification may be more likely to develop and persist in regions where bathymetry and/or stratification isolates deeper benthic regions from the oxygen-rich surface waters (Diaz, 2001; Levin et al., 2009). While the occurrence of hypoxia has been well-established in many urban estuaries, concurrent seasonal variation in pelagic carbonate chemistry has not been robustly assessed. Such characterizations are important for managing natural resources in regions that suffer from intense nutrient loading, particularly given the strong reliance of many coastal communities on calcium carbonate-secreting bivalves as primary fisheries and their sensitivity to acidification (Talmage and Gobler, 2010; Waldbusser et al., 2015; Gobler and Baumann, 2016).

Superimposed upon the seasonal dynamics of hypoxia and acidification can be intense, diurnal fluctuations in DO, pH, and carbonate chemistry (Yates et al., 2007; Hofmann et al., 2011; Frieder et al., 2012) that are modulated by biological activity and may be compounded by semi-diurnal tidal cycles (Howland et al., 2000; Frieder et al., 2012; Baumann et al., 2015; Wallace et al., 2021). Emerging research suggest these fluctuations can have negative effects on the growth and survival of early life stage finfish (Morrell and Gobler, 2020) and shellfish (Clark and Gobler, 2016; Gobler et al., 2017). While some studies have documented the short-term variability of DO and pH in coastal ecosystems, studies examining the co-evolution of hypoxia and acidification and associated changes in carbonate chemistry on short (i.e. hours) and longer (i.e. seasonal) temporal scales while concurrently evaluating spatial dynamics have not been performed.

In order to better resolve the changing conditions governing the survival and growth of carbonate-secreting fauna, the goal of this study was to quantify the temporal and spatial dynamics of hypoxia, acidification, and calcium carbonate saturation states across multiple eutrophic estuaries in the northeast US. Two of these estuaries including Long Island Sound and Jamaica Bay are well-known for the seasonal occurrence of hypoxia (Parker and O'Reilly, 1991; O'Donnell et al., 2008; O'Donnell et al., 2014), and to a lesser extent, acidification (Wallace et al., 2014). Here, vertical profiles of DO, pH, and pCO_2 were measured continuously at multiple sites to assess spatial-temporal patterns of diurnal and longer-term dynamics of hypercapnic hypoxia. Continuous measurements of DO and pH were complemented with discrete measurements of carbonate chemistry. Measurements of respiration and net ecosystem metabolism (NEM) were made to quantify processes controlling changes in water column chemistry.

2. Methods

2.1. Sampling sites

Cruises aboard the *R/V Paumanok* (Stony Brook University) were conducted in Long Island Sound (LIS), Jamaica Bay, and other neighboring estuaries from May to October to assess the seasonal, spatial, and diurnal patterns of dissolved oxygen (DO), dissolved inorganic carbon (DIC), pH, the partial pressure of carbon dioxide (pCO_2) and the saturation state of aragonite (Ω_{Ar}). During cruises, vertical profiles were performed and samples were collected using a CTD-rosette system at three locations across western LIS ranging from central LIS, north of Glen Cove, NY, a site south of Throgs Neck, NY, stations B3 (40.91167, -73.65980), A4 (40.87265, -73.74170), and A2 (40.80051, -73.78431). Vertical profiling was also performed at three locations across Jamaica Bay: the ocean-exchanging Rockaway Inlet (stations JB1; 40.63171, -73.80417, a mid-estuary site, North Channel (JB4; 40.64074, -73.85362), and the eastern extreme of the bay, Grassy Bay (J1A; 40.57285, -73.87920; Fig. 1).

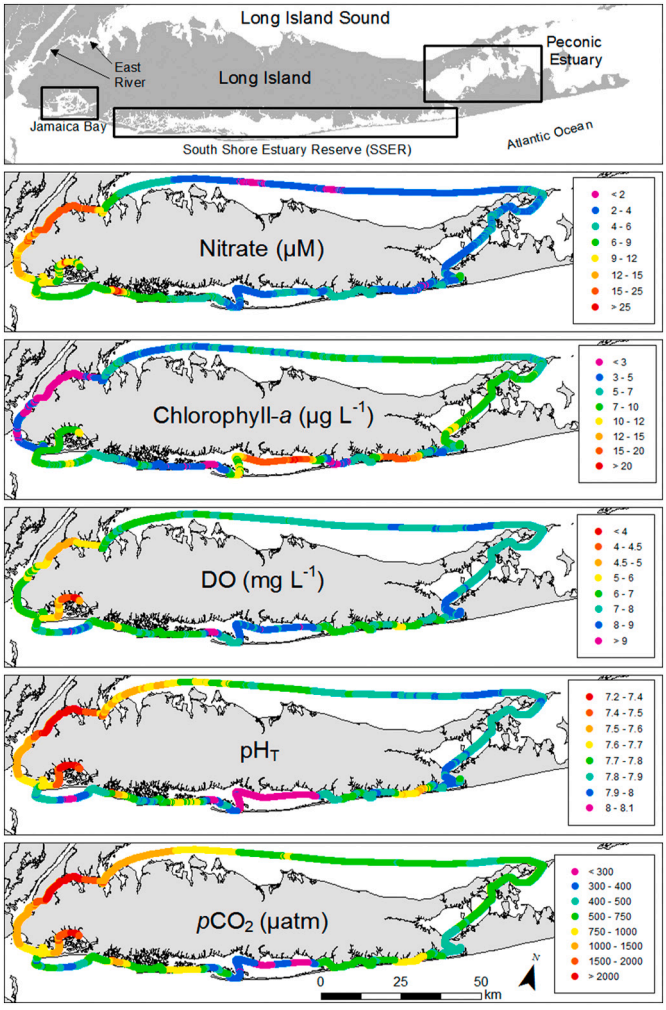

Fig. 2. High-resolution continuous surface water sampling for nitrate (μM; SUNA UV nitrate sensor), normalized chlorophyll *a* fluorescence (μg L^{-1}), dissolved oxygen (DO; mg L^{-1}), pH_T (total H^+ scale), and the partial pressure of CO_2 (pCO_2; μatm) around Long Island, New York during September 2014.

2.2. Diurnal profiling

During cruises, diurnal profiling in both Jamaica Bay and western LIS was performed every three-to-four hours over a 12 – 15-hour period from late afternoon through sunrise. This sampling periodicity was designed to capture the end of daytime, photosynthesis-driven peak of pH and DO as well as the at-dawn minimum of DO and pH expected after a night of respiration in the absence of photosynthesis. Multiple CTD casts were performed at each site using a YSI EXO2, a Contros HydroC™ CO_2 sensor, and a SeaFET pH sensor affixed to an aluminum bracket to provide continuous (0.3–1 Hz), vertical measurements of DO (mg L^{-1}), temperature (°C), conductivity (μS cm^{-1}), depth (m), pCO_2 (μatm), chlorophyll *a* fluorescence (RFU), and pH (NBS and total H^+ scale on the EXO2 and SeaFET, respectively). Discrete water samples for the direct measurement of chlorophyll *a*, pH_T (total H^+ scale), and DIC were collected from Niskin bottles retrieved from three to five depths within the water column (surface, middle, and bottom). Discrete pH samples were immediately analyzed on deck using a Honeywell DuraFET III pH (total H^+ scale) electrode integrated to a Honeywell Analytical Process Analyzer (APT) 4000pH series. DIC samples were transferred via Tygon® tubing from Niskin water samplers into 330 mL borosilicate glass BOD bottles with the sample overflowing two full volumes of water to eliminate bubbles. Samples were immediately preserved by the addition of 100 μL of a saturated mercuric chloride ($HgCl_2$) solution, sealed with a glass stopper using Apiezon L ultra-high vacuum grease, and stored at 4 °C. Poisoned DIC samples were analyzed by coulometric titration using a UIC Inc. CM5017O coulometer interfaced to a VINDTA 3D delivery system. Carbonate chemistry parameters were calculated from measured levels of DIC, pH, temperature, salinity, and the first and second dissociation constants of carbon acid in seawater (Millero, 2010) using the program CO2SYS (https://cdiac.ess-dive.lbl.gov/ftp/co2sys/). As a quality assurance measure, certified reference material generated by Dr. Andrew Dickson's lab (University of California San Diego, Scripps Institution of Oceanography) was analyzed immediately before and after sample titration and yielded full recovery during this entire study (99.99% ± 0.05).

2.3. High-resolution surface mapping

In addition to profiling the water column, a continuous flow system was developed to measure surface water characteristics at high spatio-temporal resolution when not profiling and was used to opportunistically characterize surface waters while transiting from port (Stony Brook Southampton, Marine Station, Southampton, NY) to profiling stations (Fig. 1), resulting in continuous surface measurements while circumnavigating Long Island, NY, over a ~ 500 km cruise track (Fig. 2). The continuous flow system utilized the same sensor package as described above with the addition of a Satlantic SUNA (Submersible Ultraviolet Nitrate Analyzer) nitrate (NO_3^-) sensor. The SUNA uses ultraviolet (UV; 200–400 nm) absorption spectroscopy to provide in situ measurements of dissolved NO_3^- concentrations. The water for the continuous flow system was drawn from a rigid intake 1 m below the air-sea interface via laminar flow pump. All sensor packages were integrated via custom flow cells and when integrating the Contros HydroC pCO_2 sensor, an SBE 5 T centrifugal pump was affixed in-line to maintain constant flow and reduce bubbling over the sensor membrane. A polycarbonate sleeve was attached between the pump and the HydroC to evenly displace water across the sensor membrane and maintain overflow into the sensor chamber to enable internal/external temperature equilibration (Fiedler et al., 2012; Fietzek et al., 2014). All data was transmitted at 0.3–1 Hz and georeferenced using a BU-353 S4 GPS receiver utilizing the SiRF Star IV chipset. GPS coordinates (NMEA 0183 sentences, data type; GGA, GSA, GSV, RMC, VTG, GLL, ZDA) were recorded and the output of NMEA messages was in the World Geodetic System (WGS) 1984 datum. The resulting cruise track data (georeferenced point data) was reprojected to the North American Datum of 1983 (NAD 83) and converted to Universal Transverse Mercator (UTM) zone 18 N to improve distance measurements and areal accuracy with minimal distortion. High resolution horizontal survey point was used to generate maps of each parameter using the Geostatistical Analyst extension in ArcGIS 10.4.1 (ESRI, Redlands, CA). Data collected in Jamaica Bay was interpolated using a diffusion kernel technique with an additive raster barrier. This diffusion interpolation was useful as high resolution data collected here warranted an interpolation that uses a distance metric (optimally varying kernel) that calculates the cost of travel from one cell of the matrix to the next (Krivoruchko and Gribov, 2004) and accounted for regions with insufficient data or areas that have non-transparent barriers (i.e. coastlines) for chemical propagation (Gribov and Krivoruchko, 2011). Furthermore, this interpolation was able to smooth data that was anomalous over short distances (i.e. peaks/troughs due to bubbling and/or caused by wave action moving intake vertically in the water column) that would not necessarily have been removed using a kriging method.

2.4. Discrete sample collection

Discrete surface samples were collected from the flow through system via regulation of a Y-valve between the pump and the sensor array in which excurrent water was diverted for the collection of surface samples for analysis of parameters described above. Additionally, water was filtered on deck through precombusted (2 h at 450 °C) glass fiber

filters (GF/F) and filtrate was colorimetrically analyzed for dissolved NO_3^-, nitrite (NO_2^-), ammonium (NH_4^+), and orthophosphate via a Hach QuikChem 8500 Flow Injection Analysis system (Parsons et al., 2013). Discrete chlorophyll *a* samples were collected in triplicate and filtered on deck through 0.2 μm polycarbonate filters and chlorophyll *a* was extracted and quantified using standard fluorometric techniques (Parsons et al., 2013). Extracted chlorophyll *a* samples and a linear regression model were used to normalize in situ fluorescence data ($R^2 = 0.77$; Hattenrath-Lehmann et al., 2015) and discrete measurements of NO_3^- were used to normalize continuous UV NO_3^- measurements made with the SUNA sensor (linear regression model; $R^2 = 0.88$).

2.5. Buoy array

The Department of Marine Sciences at University of Connecticut operates and maintains an array of marine monitoring platforms in LIS as part of the Long Island Sound Integrated Coastal Observing System (LISICOS; http://lisicos.uconn.edu/index.php). The two western LISICOS buoys (WLIS; 40.95583, -73.58000 & EXRX; 40.88333, -73.72833; Fig. 1) were utilized to affix a Satlantic SeaFET ocean pH sensor and were deployed with a YSI 6600 series sonde affixed with a 6150 ROX optical dissolved oxygen sensor at a depth of 21 m in a region that experiences hypoxic conditions during the summer months (May – September) enabling continuous (10 min. intervals) bottom measurements of pH_T (Fig. 1). Additionally, the three aforementioned locations across Jamaica Bay were continuously monitored with YSI EXO2 multiparameter sondes that recorded pH_{NBS}, DO (mg L^{-1}), temperature (°C), conductivity, and chlorophyll *a* fluorescence (RFU). All sensors were suspended at a depth of 3 m from fixed piers using steel cable in PVC enclosures with openings to permit extensive water flow. A second EXO2 was deployed at 7 m at the eastern most, Grassy Bay location. The sensor package at the western location near Rockaway and the Grassy Bay location (bottom only) also had a SeaFET pH sensor deployed (Fig. 1). In addition, a YSI EXO2 was also mounted to an automated, telemetered, profiling winch system affixed to a pier in Grassy Bay at JFK International Airport to enable the collection of high frequency (profiles every hour for three and five months in 2016 and 2017) and high-vertical resolution (every 10 cm over an 8 m depth) data throughout the entire water column (Fig. 1).

2.6. Net ecosystem metabolism

Ecosystem metabolism was calculated at the three Jamaica Bay sampling locations and two depths, as described above, enabling comparison of distinct metabolic rates throughout the entire field season. Diffusion of oxygen (O_{2d}) across the air-sea interface was calculated at 10 min intervals using Eq. (1) as described in Caffrey (2004) where coefficient, *k*, was estimated to be 0.5 g O_2 m^{-2} h^{-1} (Kemp and Boynton, 1980), DO_{t1} and DO_{t2} are the percent oxygen saturation at consecutive 10 min intervals, and *dt* is the time interval (h).

$$O_{2d} = [1-(DO_{t2} + DO_{t1})/200]*k*dt \quad (1)$$

For each 10 min interval, *O_2 diffusion* (O_{2d}) was subtracted from the change in DO concentrations (mg L^{-1}) multiplied by depth (*z*) of measurement (m), resulting in oxygen flux (O_{2f} g m^{-2}) as described in Caffrey, 2004 (Eq. (2)).

$$O_{2f} = \sum_{(i=1)}^{t} (DO_t - DO_{(t-1)})*z - (O_{2d}) \quad (2)$$

Estimates of daily metabolic rates were calculated by subtracting total respiration from gross production. Oxygen fluxes during daylight hours (net production) were calculated and summed oxygen fluxes at night were multiplied by -1 to determine evening respiration rates (Caffrey, 2004). Gross production and total respiration rates were estimated using net production and evening respiration values (Caffrey, 2004). Day and evening hours for all calculations were determined using daily civil twilight times (Sun is 6° below azimuth; EDT) at each sampling location assuming nighttime aerobic respiration.

2.7. Underway profiler

To complement diurnal profiles, an aluminum underway towing profiler was constructed to enable continuous vertical profiling of temperature, conductivity, DO, pH (NBS and Total H^+ scale), and chlorophyll *a* fluorescence (RFU) in Jamaica Bay. The SeaFET and the YSI EXO2 multi-parameter sonde were mounted horizontally within the towing profiler with sensors affixed to the rear of the unit to minimize turbulence and bubbling. Vertical 1/8" sheet aluminum stabilizers with a central support beam were bracketed to the top side of the unit to maintain lateral stability when traveling horizontally and vertically in the water column. A lead weight was mounted on the nose of the profiler to maintain consistent dive velocity at low speeds and a cable from the research vessel was attached to a rotational bracket. The vessel traveled at 0 - 5 knots with changes in vessel speed inducing vertical movement of the profiler within the water column. To initiate profiling, the unit was lowered to ~1 m off the bottom while the vessel was stationary and as the vessel went underway, the profiler would begin to slowly surface. The profiler depth was monitored via shipboard computer and as it approached the surface the boat engine was manually shifted to neutral allowing the profiler to descend. This process was repeated continuously across Jamaica Bay, adjusting for depth as the vessel was underway. Data collected using this profiling method was used to produce a comprehensive vertical and horizontal representation of all parameters measured, closing data gaps that would otherwise be satisfied only via extensive spatial interpolation techniques. The data generated from these cruises were superimposed over high resolution bathymetry data sets that were then integrated with high resolution LiDAR (Light Detection and Ranging) data from the surrounding coast facilitating three-dimensional viewing of the data.

2.8. Respiration rates

To complement measurements of CO_2 and DO and other parameters that can be ecosystem indicators of photosynthesis and respiration, rates of respiration of plankton communities were quantified using dark, 330 mL borosilicate glass bottles that were washed with 10% HCl, liberally rinsed with deionized water prior to use, rinsed with sample water, and filled in triplicate via Tygon tubing with seawater from various locations and depths in both Jamaica Bay and western LIS. Each bottle was filled to overflowing with two full volumes of water after which an initial DO measurement was made using a high precision, Clark electrode (polarographic sensor; YSI 5100) as described in Koch and Gobler (2009). Bottles were incubated for 12 h on deck in a chamber continuously flushed with ambient surface water, mimicking the temperature regime found in the mid-waters of Jamaica Bay and/or western LIS. After this incubation period, final DO concentrations were measured and pelagic respiration rates were determined from changes in DO levels.

3. Results

3.1. Spatial and seasonal observations across Long Island

During the summer of 2014, high-resolution surface water measurements of NO_3^- (μM), normalized chlorophyll-*a* fluorescence (μg L^{-1}), DO (mg L^{-1}), pH_T, and pCO_2 (μatm) were made across the estuaries surrounding Long Island, NY, providing a spatial assessment of conditions during the period when hypoxia and acidification arises (Wallace et al., 2014). Spatial trends across the region in September were reflective of June - August with slightly lower pH and DO and higher pCO_2 (Fig. 2). Salinity ranged from 19 to 31 across the region with the lowest values observed in the East River and maximum salinity observed along the south shore of Long Island near ocean inlets. LIS salinity

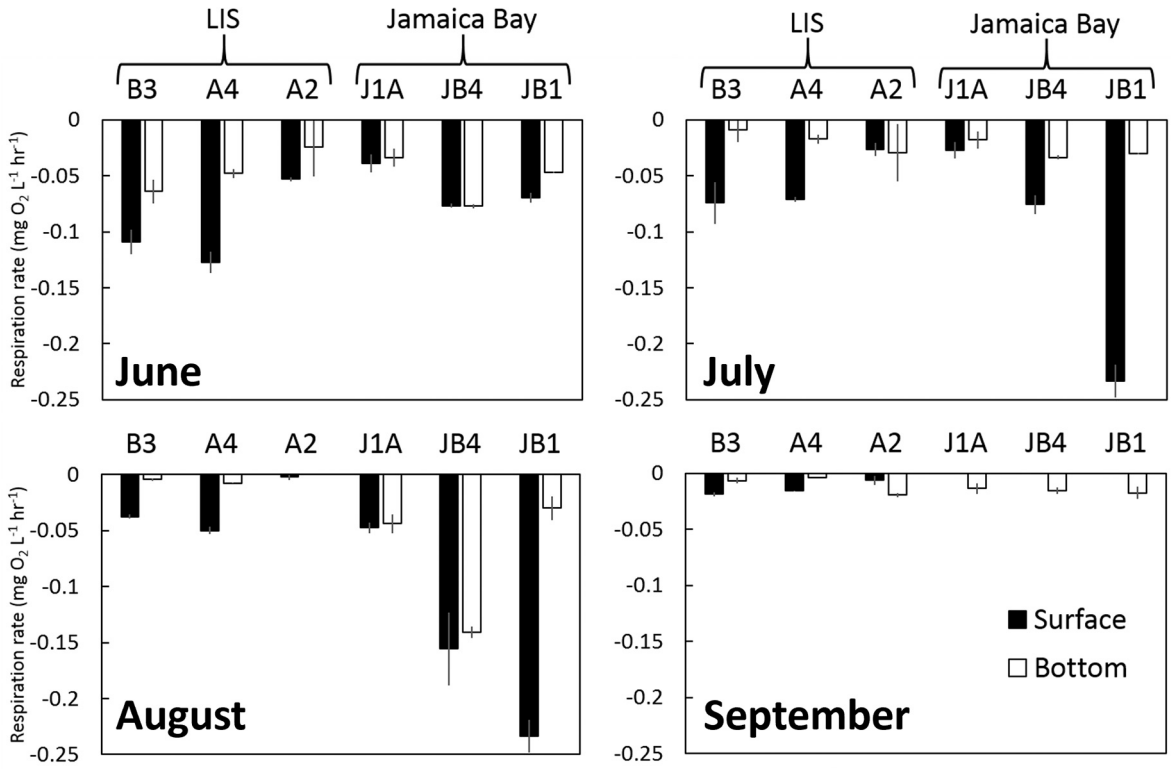

Fig. 3. Surface and bottom **r**espiration rates (mg O_2 L^{-1} h^{-1}) measured at three locations in Jamaica Bay and western Long Island Sound during June, July, August, and September. Error bars indicate ±SD of triplicate bottles.

ranged from 26 to 29 with increasing salinity to the east and lower salinity (24–26) present in Jamaica Bay and isolated parts of the South Shore Estuary Reserve (SSER). Nitrate concentrations ranged from <2–5 μM in the Peconic Estuary and eastern and central LIS, increased to 9–12 μM in western LIS, and peaked in the East River at >25 μM (Fig. 2). Nitrate levels were lower through the Hudson River and NY Bight (10-12 μM), ranged from 9 to 25 μM in Jamaica Bay, and were generally low across the SSER (1 - 10 μM; Fig. 2). A harmful 'brown tide' (*Aureococcus anophagefferens*) bloom within middle of the SSER caused elevated chlorophyll *a* concentrations (> 40 μg L^{-1}; Gobler et al., 2019) as well as high levels of DO (8–10 mg L^{-1}; Fig. 2). Regions with elevated NO_3^- and low algal biomass, including the East River, Jamaica Bay and western LIS, generally displayed lower DO concentrations (< 5 mg L^{-1}; Fig. 2), acidified conditions (pH_T = 7.2–7.6), and pCO_2 levels exceeding 2000

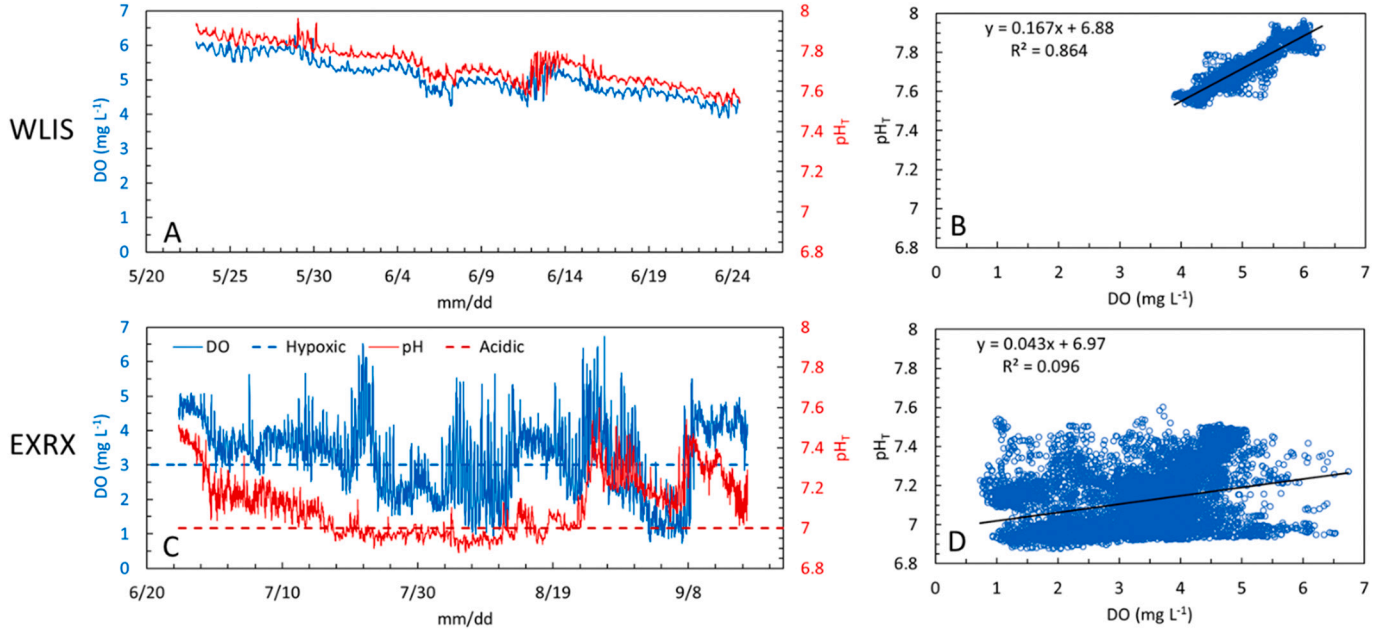

Fig. 4. Time series and paired comparisons of pH_T and DO (mg L^{-1}) at **A & B** WLIS buoy from May through June and **C & D** EXRX buoy from June through September. Both monitoring stations are maintained by University of Connecticut - Long Island Sound Integrated Coastal Observing System (LISICOS). http://lisicos.uconn.edu/

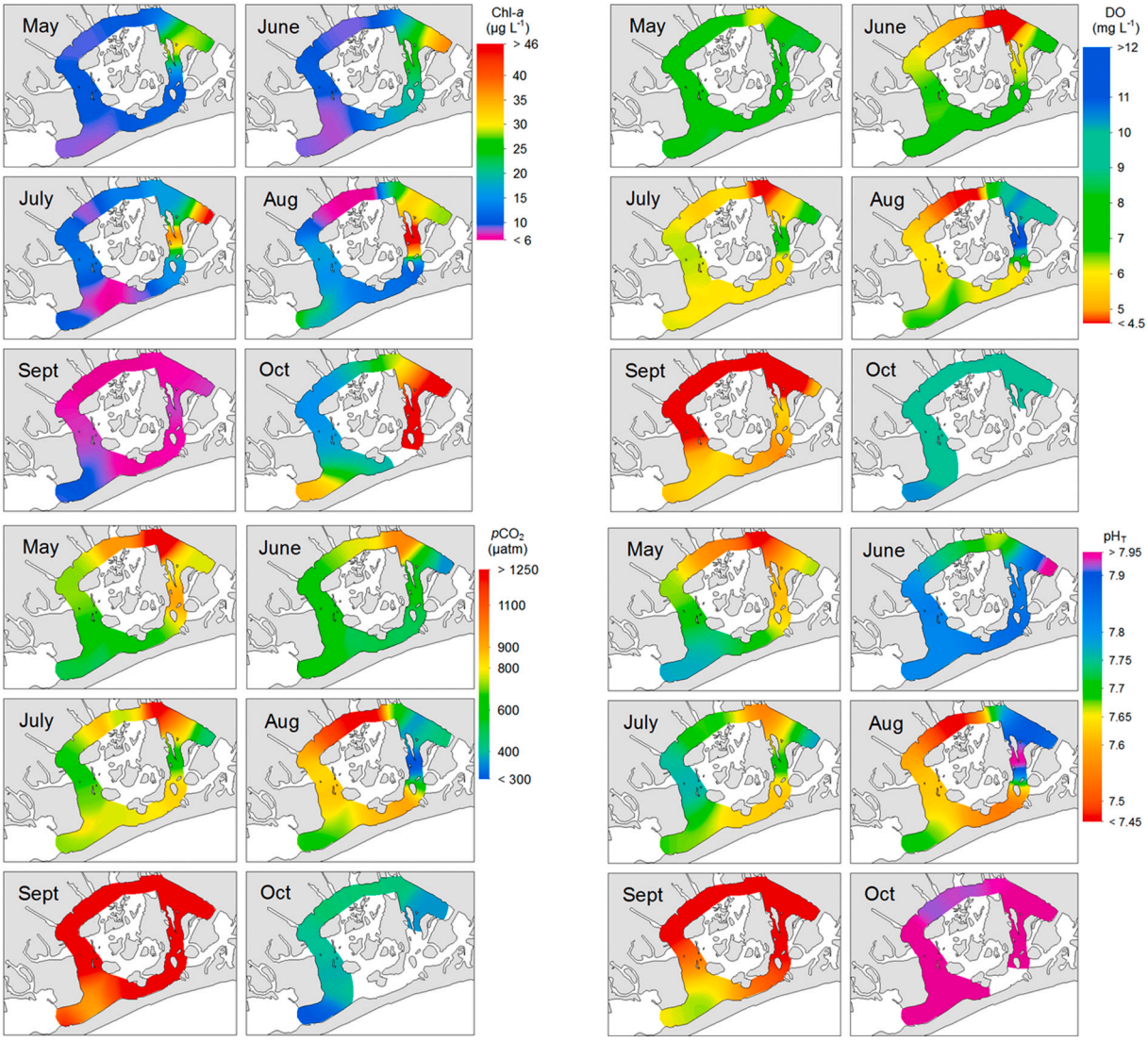

Fig. 5. High-resolution continuous surface water measurements of **top left:** normalized chlorophyll *a* fluorescence (μg L^{-1}), **top right:** DO (mg L^{-1}), **bottom left:** pCO_2 (μatm), and **bottom right:** pH_T from May – October 2015.

μatm (Fig. 2). Moving eastward from these sites, pH levels rose to 7.8-7.9 and pCO_2 decreased to 500–750 μatm across eastern LIS and the Peconic Estuary (Fig. 2). Levels of pH and pCO_2 were dynamic across the SSER with elevated pH_T (8–8.1) and a drawdown in pCO_2 (< 300 μatm) in some regions during the brown tide bloom (Fig. 2). This and other cruises collectively demonstrated that across the ~500 km cruise track, Jamaica Bay and western Long Island Sound were the regions most prone to low DO, low pH and high pCO_2 levels in surface waters (Fig. 2) and thus were focal areas of this study.

3.2. Respiration rates in LIS and Jamaica Bay

During the summer of 2014, respiration rates were measured in surface and bottom waters at six locations that displayed low pH and DO in western LIS ($n = 3$) and three locations in Jamaica Bay ($n = 3$; Fig. 1). In LIS, respiration rates were highest in June at stations B3 and A4 exceeding 0.1 mg O_2 L^{-1} h^{-1} but declined each month thereafter with surface water respiration rates always exceeding respiration rates at depth (Fig. 3). In Jamaica Bay, respiration rates were highest at the North Channel site (JB4) within Jamaica Bay, with no difference between surface and bottom (Fig. 3), whereas in Grassy Bay (JB1), surface respiration rates were higher than bottom respiration rates ($p < 0.05$; Tukey test; Fig. 3). Respiration rates were significantly lower at the ocean inlet (J1A) than all other sites in Jamaica Bay ($p < 0.05$; Tukey test) with no difference between surface and bottom rates (Fig. 3). While respirations rates for all sites in Jamaica Bay were modest in June and September (< 0.1 mg O_2 L^{-1} h^{-1}), rates were significantly higher in July and August, particularly within the surface waters of Grassy Bay which exceeded 0.2 mg O_2 L^{-1} h^{-1} and were significantly higher than bottom waters there and surface or bottom water rates at all other sites ($p < 0.05$; Tukey test; Fig. 3).

3.3. Dynamics of DO and pH in LIS bottom waters during summer

Given the high rates of respiration and low oxygen and pH conditions in western LIS, the relationship between DO and pH was examined in the bottom waters via sensor deployments during the summer of 2014. During a May through June deployment in western LIS, pH_T declined from 7.9 to 7.6, DO declined from 6 to 4 mg L^{-1} and the two parameters were strongly correlated ($R^2 = 0.86$; Fig. 4A&B). The sensors were then moved ~15 km southwest at the end of June (Fig. 1; EXRX). Levels of pH_T and DO steadily declined from 7.5 and 5 mg L^{-1}, respectively, in late June to 7.1 and 3 mg L^{-1} in early July (Fig. 4C). From mid-July through mid-August, pH_T reached and maintained acidic levels (< 7) while DO

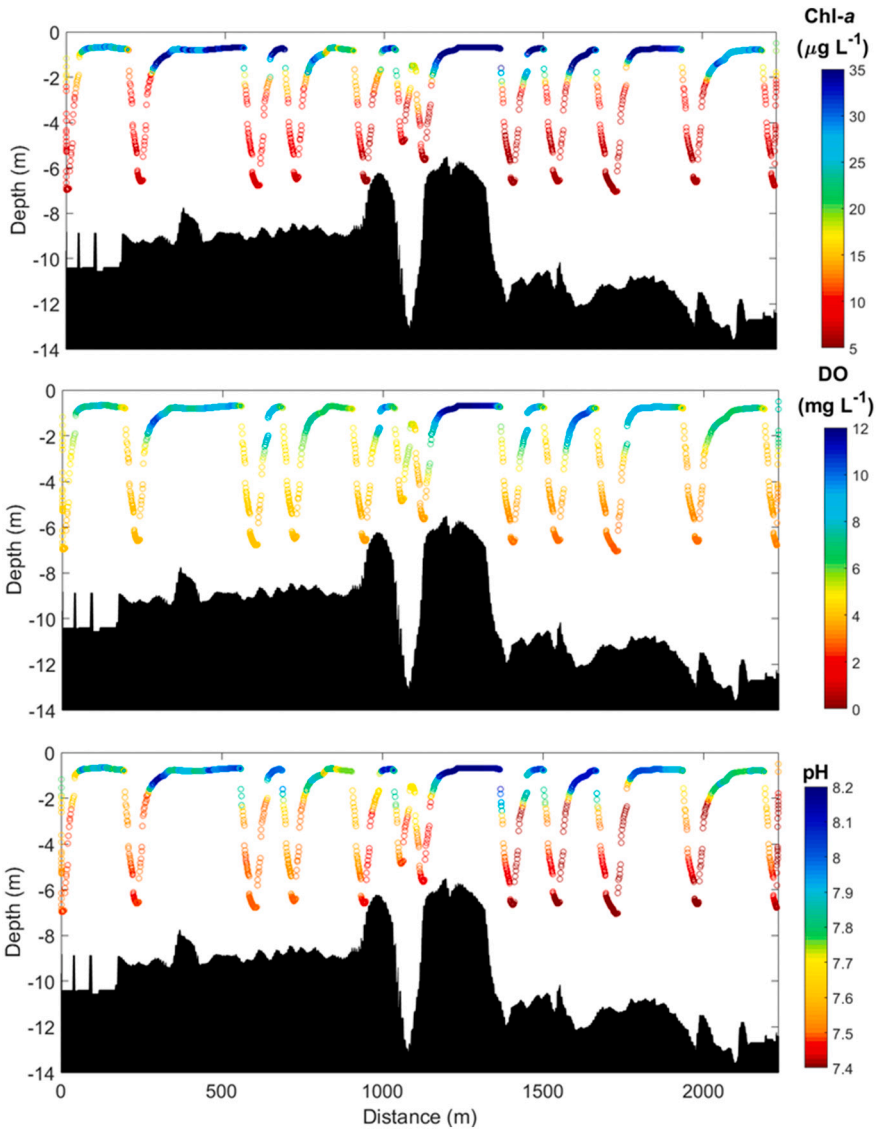

Fig. 6. High-resolution vertical section plots of **top:** normalized chlorophyll *a* fluorescence (μg L^{-1}), **middle:** DO **(mg L^{-1})**, and **bottom:** pH_{NBS} in Grassy Bay during August 2015. Data was collected using a continuous underway towing profiler. See links below for full animations. See Supplementary Fig. S1 for animation screenshots.
A) Chlorophyll; https://www.youtube.com/watch?v=06HG386oCM0&t=1s.
B) DO; https://www.youtube.com/watch?v=LcFNybC867M.
C) pH; https://www.youtube.com/watch?v=VDXKO6raSUI.

was more dynamic with nightly minimums that were often hypoxic (< 3 mg L^{-1}) but also strong diurnal fluctuations through mid-August (Fig. 4C). In late August, pH levels rose above 7.1 for the first time in ~40 days and fluctuated between 7.1 and 7.5 in parallel with DO which varied between 1 and 8 mg L^{-1} through the end of the deployment in mid-September (Fig. 4C). In contrast to the late spring deployment in western LIS, pH and DO at EXRX were poorly correlated during summer ($R^2 = 0.10$; Fig. 4D).

4. Fine scale assessment of acidification and hypoxia in Jamaica Bay

Given the highly eutrophic nature of Jamaica Bay (Figs. 2 & 3), high resolution surface water surveys of chlorophyll *a*, DO, pCO_2, and pH_T were performed monthly from May through October of 2015. During the first half of the surveys (May, June, July), similar spatial patterns persisted with chlorophyll *a* levels being low through much of the system (< 5 μg L^{-1}), except for Grassy Bay (Fig. 1; JB1) in the northeast where levels exceeded (40 μg L^{-1}; Fig. 5). DO levels were ~ 8 mg L^{-1} for much of the Bay in May and June and declined to 6 mg L^{-1} during July but were lower in the northeast corner of the Bay (6 mg L^{-1} in May; < 4.5 mg L^{-1} in June and July; Fig. 5). Patterns of pCO_2 and pH paralleled DO during this period with pCO_2 levels being 500–800 μatm for most of the Bay from May through July with peaks near or exceeding 1000 μatm appearing each month in the North Channel (Fig. 1; JB4) where pH_T was also low (<7.65; Fig. 5). In August in North Channel, DO concentrations decreased to 4 mg L^{-1} as pCO_2 levels exceeded 1200 μatm and pH_T decreased to 7.4, whereas a dense surface algal bloom (chlorophyll *a* > 50 μg L^{-1}) in Grassy Bay increased DO and pH to 12 mg L^{-1} and 8, respectively, while decreasing pCO_2 to <300 μatm (Fig. 5). Vertical sampling in August revealed this algal bloom and its influence on water chemistry was restricted to the upper 4 m as chlorophyll *a* concentrations decreased to <5 μg L^{-1} below 4 m where hypoxic (DO <3 mg L^{-1}) and acidified conditions (pH_{NBS} < 7.4) persisted (Fig. 6, Supplementary Fig. S1). In contrast, western and southern channels of the bay had levels of chlorophyll *a* (10-15 μg L^{-1}), DO (5 -7 mg L^{-1}), and pH_{NBS} levels (7.5–7.6) that were higher with little evidence of vertical stratification of pH, DO, and chlorophyll *a* (Fig. 6). In September, North Channel and Grassy Bay had DO concentrations <4 mg L^{-1} while the rest of the bay had concentrations between 5 and 6 mg L^{-1} and pCO_2 increased to >1500 μatm and pH_T decreased <7.4 throughout most of the bay, with the exception of the Inlet, where pCO_2 levels were 800 - 1000 μatm and pH_T was 7.7 (Fig. 5). Finally, in October, chlorophyll *a* levels increased, DO rose to above 10 mg L^{-1} throughout the bay, pCO_2 levels dropped to below 400 μatm and pH_T exceeded 7.9 (Fig. 5).

In 2015, high frequency (~10 min sampling intervals) monitoring

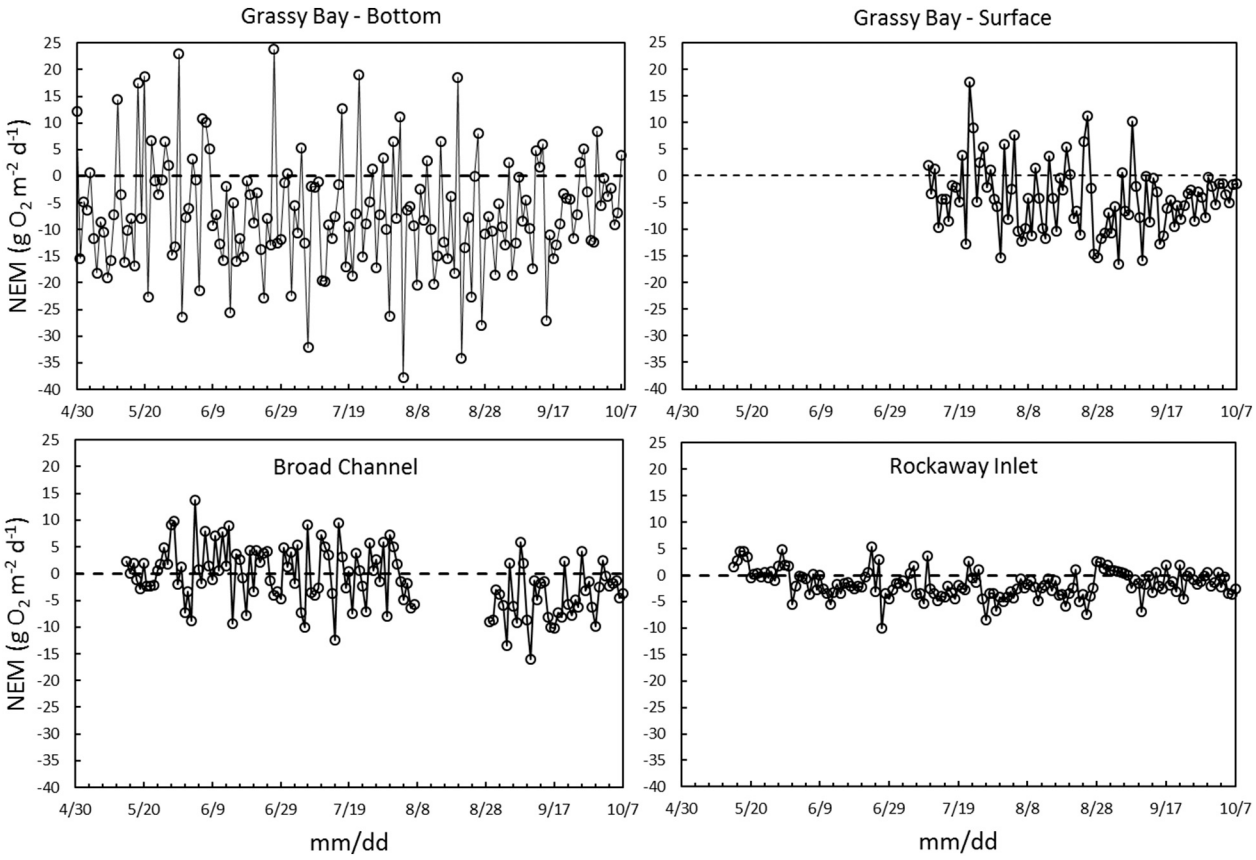

Fig. 7. Daily net ecosystem metabolism (NEM; g O_2 m^{-2} d^{-1}) in Grassy Bay bottom waters (top left), Grassy Bay surface waters (top right), Broad Channel (bottom left), Rockaway Inlet (bottom right), April – October 2015.

arrays were deployed from May through October across the eutrophication gradient within Jamaica Bay (Inlet, mid-bay, Grassy Bay to the east; Fig. 1) to assess fine scale temporal fluctuations in DO, pH, and chlorophyll *a* and to quantify NEM. Surface waters of Grassy Bay (Fig. 1; JB1) were strongly net heterotrophic (NEM = -4.12 ± 5.59 g O_2 m^{-2} d^{-1}) through most of the year with brief periods of net autotrophy in the summer coincident with ephemeral algal blooms (Fig. 7). NEM was substantially more negative in bottom waters of Grassy Bay (-8.66 ± 11.75 g O_2 m^{-2} d^{-1}; Fig. 7). The central region of Jamaica Bay was more balanced with a mean metabolic rate of -1.2 ± 5.6 g O_2 m^{-2} d^{-1} with net heterotrophic conditions becoming more prominent later in the season (Fig. 7). The inlet region was also net heterotrophic but exhibited less variability than other sites, with mean metabolic rates of -1.48 ± 2.58 m^{-2} d^{-1} (Fig. 7).

Linear regressions of DO and pH_{NBS} plotted with chlorophyll *a* levels from the 2015 deployments revealed strong and significant correlations in Broad Channel (R^2 = 0.72; $p < 0.0001$), Grassy Bay (surface R^2 = 0.51; bottom R^2 = 0.49; $p < 0.0001$ for both), and Rockaway Inlet (R^2 = 0.42; $p < 0.0001$) between DO and pH (Fig. 8). High pH and DO conditions were coincident with algal blooms (> 30 μg chlorophyll *a* L^{-1}) and low chlorophyll *a* conditions often coincident with hypoxic and acidified conditions (Fig. 8). Bottom waters of Grassy Bay were sampled over 21,000 times and both acidified and hypoxic conditions (pH < 7.6; DO <3 mg L^{-1}) were present 52% of the time whereas at the surface, acidified and hypoxic conditions occurred 13% and 11% of the time (n = 12,789), respectively (Table 1). In contrast, stations in the central bay (n = 17,144) and inlet (n = 20,151) were acidified and hypoxic 7% and < 1% of the time, respectively (Table 1).

To assess diurnal patterns of DO, pH_T, pCO_2, and Ω_{Ar} within Grassy Bay (Fig. 1; JB1), vertical profiles were performed from late afternoon through the early morning hours from June through September. In June, diurnal changes were mild (Fig. 10). DO was elevated in surface waters (> 9 mg L^{-1}) and lower (< 5 mg L^{-1}) below 8.5 m during the late afternoon, while pH_T was 8.2 at the surface and 7.8 at the bottom (Fig. 9). Both pCO_2 and Ω_{Ar} were relatively constant over the entire sampling period as pCO_2 ranged from 400 to 600 μatm and Ω_{Ar} ranged from 1.5–2.5 in surface waters with undersaturated conditions in bottom waters (Fig. 9: $\Omega_{Ar} < 1$). In July, stronger diurnal changes were observed as DO decreased in the surface waters through the night (Fig. 9) while pCO_2 increased from 400 μatm in the mid-afternoon to 1000 by dawn resulting in aragonite undersaturation throughout the entire water column (Fig. 9; $\Omega_{Ar} < 1$). By August, a dense phytoplankton bloom (chlorophyll *a* was >50 μg L^{-1}) created supersaturated DO conditions (>11 mg L^{-1}), lower pCO_2 (< 500 μatm), elevated pH_T (>8.1), and saturation with respect to aragonite ($\Omega > 2.5$) in surface waters in the afternoon with hypoxic (< 3 mg L^{-1}), acidified ($pH_T < 7.3$), high pCO_2 (> 2500 μatm), and undersaturated conditions present ($\Omega < 0.5$) at depth (> 8 m; Fig. 10). Through the night, this zone of acidified and hypoxic water migrated upward to encompass most of the water column (Fig. 9). In September, while dissolved oxygen was saturated (DO >8 mg L^{-1}) and pH was moderate (pH ~ 7.8) in surface waters in the late afternoon, at dawn DO and pH decreased to <4 mg L^{-1} and < 7.3 across the entire water column (Fig. 9). Concurrently, Ω_{Ar} and pCO_2 in surfaced waters transitioned from >1 and ~ 1000 μatm, respectively, in the afternoon to unsaturated conditions ($\Omega < 0.5$) and > 2500 μatm throughout the entire water column by dawn (Fig. 9).

Finally, during summer and fall of 2016 and 2017, an automated, telemetered, winch in Grassy Bay recorded fine scale vertical and temporal dynamics of pH, DO, and chlorophyll *a*. In early August of 2016, a dense phytoplankton bloom occurred with chlorophyll *a* > 50 μg L^{-1} while DO concentrations exceeded 12 mg L^{-1} and pH_{NBS} exceeded 7.8 through most of the water column (Fig. 10). Following this event,

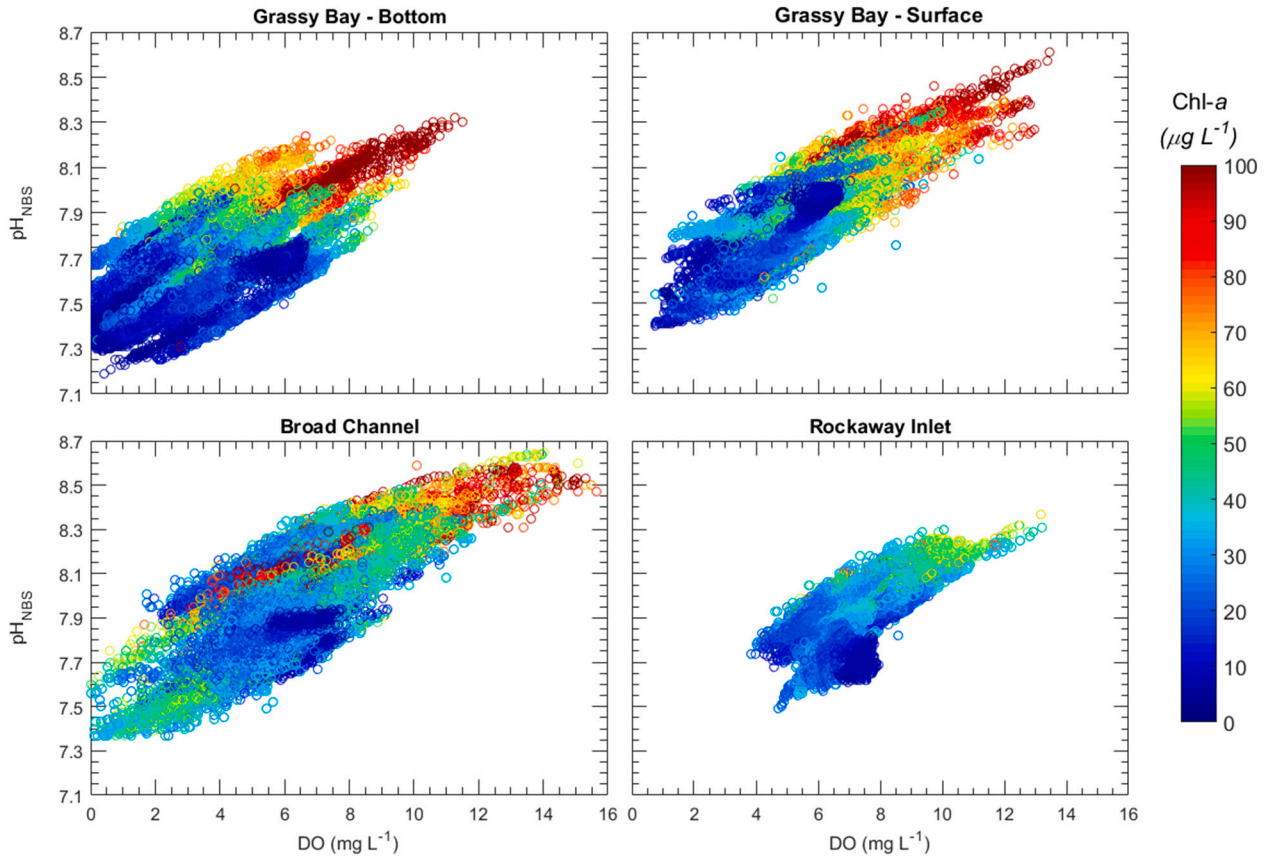

Fig. 8. Linear regressions of pH_{NBS} and DO (mg L^{-1}) plotted with normalized chlorophyll *a* fluorescence (colormap) in Grassy Bay bottom waters (top left), Grassy Bay surface waters (top right), Broad Channel (bottom left), and Rockaway Inlet (bottom right), April – October 2015. Sites are identical to Fig. 8.

Table 1
Percentage of high-frequency pH measurements <7.4, < 7.6, and < 7.8 and DO measurements <2, 3, and 5 mg L^{-1} at sites RL, BC, and JFK surface and bottom. Far right column indicates total number of samples (n).

Site	pH < 7.4	pH < 7.6	pH < 7.8	DO < 2	DO < 3	DO < 5	Total Samples
RL	0	0.27	13.57	0	0	4.64	20,157
BC	0.3	6.71	22.91	2.21	6.31	26.69	17,144
JFK Surf	0.02	13.35	47.9	2.64	11.48	46.17	12,789
JFK bot	12.77	51.54	82.19	31.94	52	79.71	21,227

chlorophyll *a* levels declined by an order of magnitude and the entire water column became acidified (pH < 7.6) with DO at 5 mg L^{-1} in surface waters and < 3 mg L^{-1} at depth (Fig. 10). In early September, a second, smaller algal bloom (chlorophyll *a* ~ 20 μg L^{-1}) increased DO and pH_{NBS} in surface waters, while bottom waters remained hypoxic (< 3 mg L^{-1}) with pH < 7.4 (Fig. 10). After this second bloom, the entire water column again reverted to a state of low DO (< 5 mg L^{-1}) and low pH (<7.5; Fig. 10). This general pattern repeated with small blooms in late September and early October that temporarily increased surface pH_{NBS} and DO while bottom waters remained hypoxic and acidified until late October when the DO and pH_{NBS} over the entire water column to rose to >8 mg L^{-1} and > 7.9, respectively (Fig. 10).

In 2017, similar patterns emerged. Ephemeral algal blooms (2–5 days of chlorophyll *a* > 10 μg L^{-1}) occurred approximately every two-to-three weeks, temporarily raising DO and pH_{NBS} in surface waters while hypoxic and acidified conditions persisted in bottom waters. Exceptions to this pattern were high DO (>5 mg L^{-1}) and pH (>7.9) levels that penetrated to the bottom in June and low DO (<3 mg L^{-1}) and low pH (<7.7) conditions that were spread through the entire water column in August (Fig. 10).

5. Discussion

This study documented the dynamic patterns of chlorophyll *a*, DO, pH, pCO_2, and Ω_{Ar} that evolve vertically, horizontally, diurnally, and seasonally across eutrophic estuaries. The spatial and temporal coherence of chlorophyll *a*, DO, and carbonate chemistry demonstrated the central role of primary production regulating DO and carbonate chemistry across the water column. Coastal systems that suffer from acute anthropogenic eutrophication can be especially vulnerable to hypoxia and acidification (Sunda and Cai, 2012; Wallace et al., 2014; Laurent et al., 2018) and these anthropogenic processes can further intensify both spatial and temporal variance (Bauer et al., 2013; Baumann and Smith, 2018). This study provides novel insight into the fine-scale dynamics of, and the processes driving, hypoxia and acidification in eutrophic estuaries.

Phytoplankton blooms strongly influenced the dynamics of DO and carbonate chemistry during this study. Excessive loading of nitrogen and phosphorus can stimulate the growth of phytoplankton and intense algal blooms in estuaries with limited tidal exchange (Paerl et al., 2014a) including LIS (Gobler et al., 2006) and Jamaica Bay (Wallace and Gobler, 2015). The initiation of algal blooms during this study led to

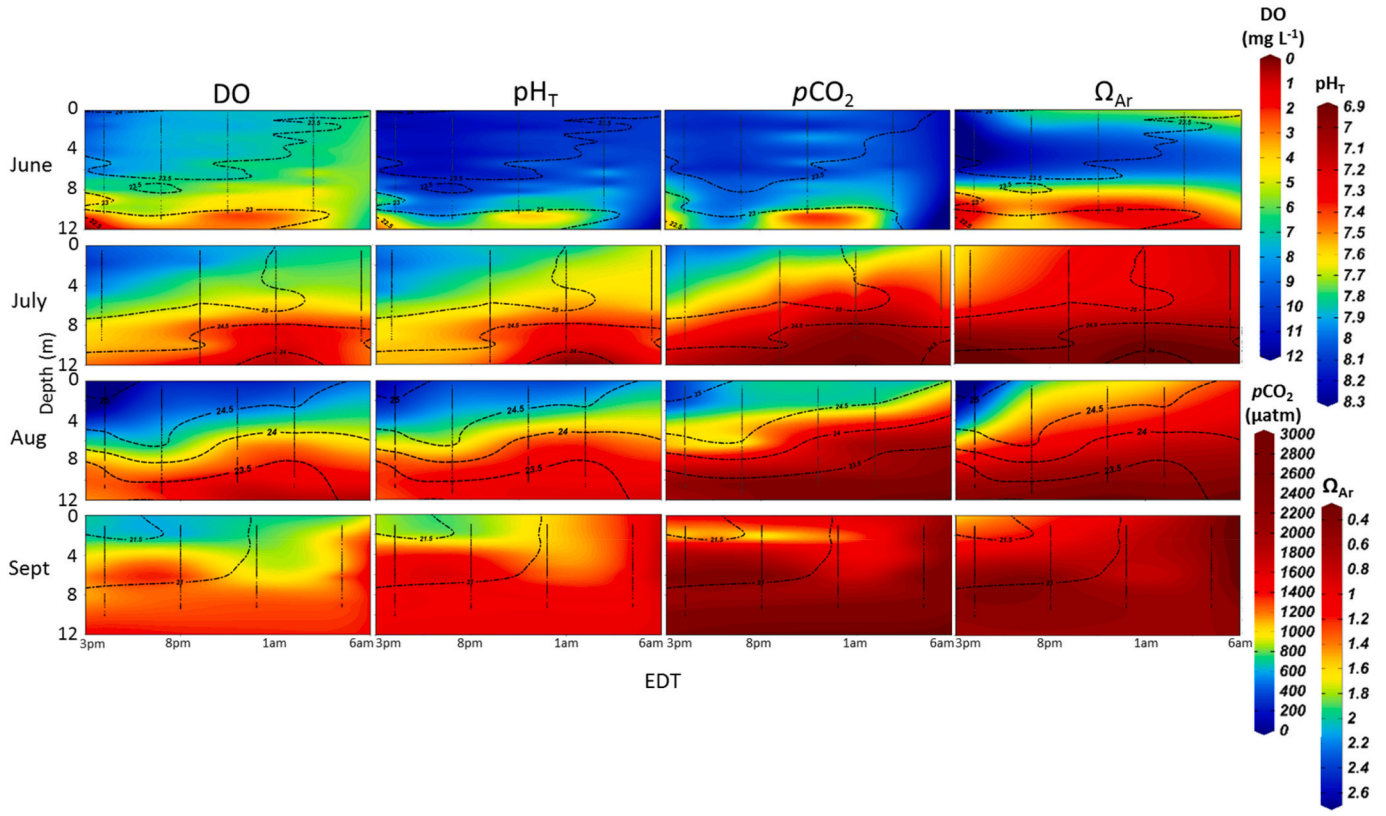

Fig. 9. Vertical section plots of DO (mg L^{-1}), pH_T, pCO_2 (µatm), and Ω_{Ar} with temperature (°C) contours at station JB1 in Grassy Bay during June, July, August, and September 2014. Vertical profiles were performed four times over a 12–15 h period from mid-afternoon through the early morning hours (EDT) as indicated by the horizontal axis.

supersaturation of DO and basification of surface waters, conditions that typically did not penetrate into deeper regions and were ephemeral (< one week). Subsequent respiration of that primary production can decrease DO concentrations, increase CO_2, and acidify estuaries (Sunda and Cai, 2012; Wallace et al., 2014; Breitburg et al., 2018), an occurrence that was observed seasonally and diurnally during this study. In addition, water bodies with minor or even undetectable physical stratification often displayed strong chemical stratification with supersaturated DO conditions and basification in productive surface waters overlaying hypoxic and acidified bottom waters. Superimposed on the ephemeral impacts of algal blooms during this study was a progressive seasonal increase in pCO_2 coupled with seasonal declines in pH and DO as the intensity and extent of acidified and hypoxic regions expanded from spring through fall. By late summer and early fall, hypoxic conditions (< 3 mg L^{-1}) were prevalent and pCO_2 exceeded 2000 µatm in both systems studied here.

The strong influence of phytoplankton blooms on DO and carbonate chemistry was also evident in shallower systems during this study. For example, both Jamaica Bay and GSB experienced periods of elevated DO concentrations (> 10 mg L^{-1}) and depressed pCO_2 levels (< 300 µatm) and dense algal biomass (chlorophyll a > 30 µg L^{-1}) during summer months partly associated with extended residence times (Gobler et al., 2019). Dense phytoplankton blooms in shallow coastal systems can often increase DO, and depress CO_2 well below saturation causing pH and Ω_{Ar} to increase (Cotovicz et al., 2018). These biologically driven seasonal shifts in carbonate chemistry and DO can be common in shallow temperate and subtropical estuaries (Murrell et al., 2018; Shadwick et al., 2019), and these transitions can be further compounded by allochthonous nutrient input (Kemp et al., 2005; Barnes and Raymond, 2009). Wastewater was the dominant nitrogen source driving eutrophication of systems studied here. In Jamaica Bay and LIS, dozens of sewage treatment plants discharge billions of liters of treated sewage into surface waters (O'Shea and Brosnan, 2000; Benotti et al., 2007) whereas the dominant source of N to the SSER is groundwater enriched in N from on-site septic systems (Kinney and Valiela, 2011).

While diurnal variability in DO and carbonate chemistry has been examined in many coastal systems (Burnett, 1997; Yates et al., 2007; Frieder et al., 2012; Baumann et al., 2015; Cyronak et al., 2018), studies of the vertical dynamics of DO and carbonate chemistry over diel timescales have been rare. Strong diurnal variability in DO and pH have been observed in highly productive temperate coastal systems (Baumann and Smith, 2018) and deeper eutrophic estuaries exhibiting high primary production in surface waters can be more vulnerable to seasonal hypoxia at depth (Levin et al., 2009; Shen et al., 2019). Furthermore, as seasonal hypoxia intensifies in bottom waters, acidification and hypoxia may expand into surface waters on diel timescales (Tyler et al., 2009; Schulz and Riebesell, 2013). This was clearly observed from July through September in Jamaica Bay where surface waters supersaturated in DO and calcium carbonate transitioned to hypoxic and acidified at night resulting in undersaturation of calcium carbonate throughout the entire water column. These diel transitions are likely to have important biological implications (see *Biological Implications* below) and may be important when considering the creation of more environmentally realistic experimental designs in future ocean acidification research (Cornwall and Hurd, 2016).

Absent pulses of intense primary production, the systems studied here were dominated by heterotrophic processes. Peak respiration rates measured (0.25 mg O_2 L^{-1} h^{-1}) during this study were exceedingly high in comparison to measurements made in other temperate coastal systems (Elena García-Martín et al., 2011; Tait and Schiel, 2013; Murrell et al., 2018). Similar, nearly all measurements of NEM in Jamaica Bay were negative with mean rates for the Grassy Bay being lower than 42 other estuaries surveyed across the US (Caffrey, 2004). Under such strongly net heterotrophic conditions, DIC and CO_2 concentrations

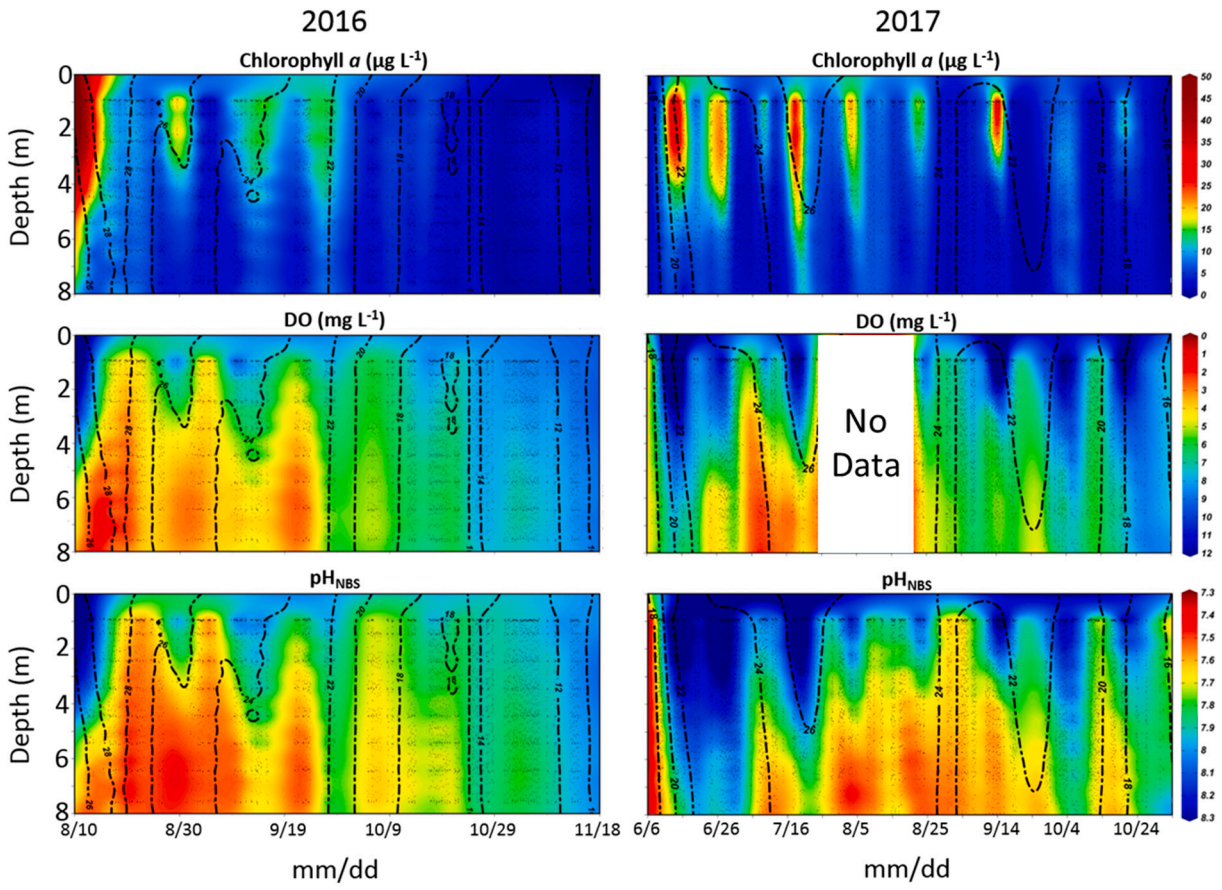

Fig. 10. Vertical section plots of normalized chlorophyll *a* fluorescence (µg L^{-1}), DO (mg L^{-1}), and pH_{NBS} with temperature (°C) contour lines at the JFK station in Grassy Bay from August – November 2016 and June – October 2017. Data was collected using an automated, telemetered profiler and stippling represents sampling points.

increase and CO_3^{-2} declines (Schulz and Riebesell, 2013), a pattern commonly observed in western LIS and Jamaica Bay where bottom waters experienced chronically low pH (< 7.5), high levels of pCO_2 (> 1500 µatm), and aragonite undersaturation (Ω < 1) representing some of the clearest examples of coastal ocean acidification (Wallace et al., 2014). These rates also drive hypoxia which persisted for more than 40

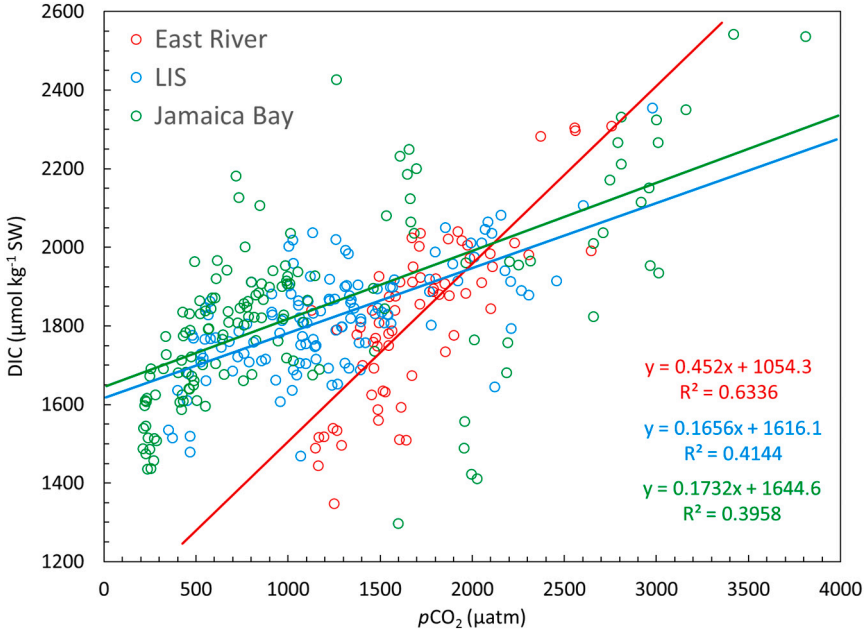

Fig. 11. All paired measurements of DIC (µmol kg^{-1}) and pCO_2 (µatm) in the East River (red), Long Island Sound (blue), and Jamaica Bay (green). (For interpretation of the references to colour in this figure legend, the reader is referred to the web version of this article.)

days in the bottom waters of western LIS and Jamaica Bay.

Eutrophic lagoons may be highly susceptible to hypoxia and acidification as nutrient loads are retained and recycled due to restricted ocean water exchange (McGlathery et al., 2007; Paerl et al., 2014b). This was clearly the case across Jamaica Bay where the ocean inlet (Rockaway Inlet) in the southwest corner had moderate DO and pH levels that contrasted strongly with the eastern, Grassy Bay region which receives the largest nutrient loads, has the longest residence times, and has some of the deepest and most stratified regions in Jamaica Bay (Benotti et al., 2007; Marsooli et al., 2018) contributing to the persistence of hypoxia and acidification within bottom waters (Wallace et al., 2014). Low DO, low pH, high pCO_2, and low Ω_{Ar} were present in the bottom 4 m of the water column of Grassy Bay as early as June and persisted through September each year. Intense algal blooms often occurred in surface water during July and August increasing the pH_{NBS} by 0.8 in surface waters (7.5 ➔ 8.3) while increasing DO concentrations by up to 7 mg L^{-1} (5 ➔12 mg L^{-1}), oxygenating the surface waters and buffering against acidified conditions (Wallace et al., 2014). Furthermore, while algal blooms were capable of maintaining high DO and pH levels for up to a week, when such blooms collapsed, hypoxic and acidified conditions developed throughout the water column. These conditions contrasted with those within North Channel and the Rockaway Inlet that experience minimal stratification and stronger tidal flow (Gordon et al., 2001) and thus were more resistant to severe and/or extended periods of hypoxia and acidification.

In contrast to regions strongly influenced by respiration-driven coastal ocean acidification, the highest pCO_2 levels and lowest pH and DO concentrations in surface waters were consistently observed within the East River. This region also had DIC concentrations that were paradoxically low relative to pCO_2 (Fig. 11) suggesting a process beyond respiration was acting on the carbonate system. One mechanism that could create these conditions would be high ammonification and nitrification rates in the absence of denitrification (Rysgaard et al., 1996). The East River receives over 3.8 billion liters of treated effluent per day from six sewage treatment facilities serving over 4.2 million residents (NYCDEP, 2004). Wastewater discharge from these facilities and CSO events can cause increased NH_4^+ and organic-N concentrations in coastal systems (Bruesewitz et al., 2017; McLaughlin et al., 2017) and the East River has been known to harbor exceedingly high concentrations of both organic and dissolved inorganic nitrogen (Chen et al., 1975; Gobler et al., 2006). In addition, the East River had the lowest TA, lowest chlorophyll *a* concentrations, highest NO_3^- concentrations, and lowest respiration rates observed during this study, likely due, in part, to the strong tidal flushing of this narrow tributary (Li et al., 2018). Ammonification of sewage-derived organic-N would increase CO_2 concentrations and increase NH_4^+ concentrations, while high rates of nitrification would consume oxygen, increase H^+ concentrations, and decrease both total alkalinity (TA) and pH (Doney et al., 2007). With minimal planktonic biomass present to assimilate excess NO_3^- and oxic conditions inhibiting denitrification (Rysgaard et al., 1994), the East River likely suffers from acidification wrought from nitrification. Increased microbial nitrification will subsequently reduce alkalinity (Doney et al., 2007) and since the East River had the lowest salinity water of all estuaries surrounding Long Island (~22), the resulting low TA creates in a lower buffering capacity, further exacerbating acidification.

Another region influenced by processes beyond primary production and respiration was the bottom waters of LIS. During the extended monitoring of pH_T and DO in western LIS bottom waters, levels of both parameters progressively declined through spring as respiration rates increased. During summer, however, DO and pH_T in bottom water began to decouple as DO became highly dynamic (1–6 mg L^{-1}) but pH remained low and somewhat static (6.9–7.1) for over a month during which these parameters were poorly correlated ($R^2 = 0.1$), suggesting processes beyond respiration were influencing pH. Oxidation reactions in surface sediments can produce strong acids that lower pH in bottom waters (Green et al., 1998; Soetaert et al., 2007) and under oxic conditions, mineralization and oxidation of reduced substances including HS^-, NH_4^+, Fe^{2+}, and Mn^{2+} may reduce pH (Aller, 1990; Soetaert et al., 2007). Spikes in bottom DO were common during this period and the reoxidation of anaerobic metabolites may utilize available DO (Aller, 1990) and produce H^+, decreasing TA, and acidifying the water above (Cai et al., 2017). In western LIS, it seems that these combined processes (aerobic respiration and oxidation of anaerobic metabolites) seasonally depressed Ω_{Ar} in bottom waters as all bottom water measurements of Ω_{Ar} in LIS were < 1 from June through September during this study.

5.1. Biological implications

Many of the conditions observed during this study have elicited harmful effects in marine animals within experimental settings. Reductions in saturation state of calcium carbonate, Ω, can have deleterious effects on benthic mollusks (Gazeau et al., 2013), especially larval stages (Waldbusser et al., 2015; Ramesh et al., 2018). Although the surface waters within much of western LIS and Jamaica Bay remained saturated with respect to aragonite for most of this study, extended periods of unsaturation in bottom waters were common and could threaten early life stage bivalves (Talmage and Gobler, 2010, 2011; Gazeau et al., 2013) and potentially depress populations (Grear et al., 2020). The seasonal intensity of acidification within these ecosystems ($pH < 7.5$, $pCO_2 > 2000$ μatm, $\Omega_{Ar} < 0.5$) exceeds future projections of open ocean acidification (Doney et al., 2012) and falls within the levels that reduce the growth and survival of calcifying bivalves (Kroeker et al., 2010; Kroeker et al., 2013; Gobler et al., 2014), crustaceans (Long et al., 2013; Tomasetti et al., 2018) and finfish (Baumann et al., 2012; DePasquale et al., 2015). Although the surface waters and shallower regions of the eutrophic estuaries examined here had levels of DO and pH supportive of marine life by day, they often transitioned into hypoxia and hypercapnia at night. Such diurnal cycles in low DO and acidification has been shown to inhibit the growth and survival of early life stage bivalves and finfish (Clark and Gobler, 2016; Gobler et al., 2017; Morrell and Gobler, 2020). In the bottom waters of Grassy Bay, hypoxic (DO <3 mg L^{-1}) and acidified ($pH < 7.6$) conditions were observed >50% of the time ($n = 21{,}227$) from April - October. While Jamaica Bay is a region in which bivalve restoration has been examined as one approach to reducing planktonic biomass as a means for improving water quality (Levinton and Doall, 2019), extended periods of hypoxia and acidified conditions may impede bivalve restoration efforts within this system. Future estuarine management approaches will need to consider the short and longer term occurrence of hypoxia and acidification and will need to consider restoration within regions that can provide habitat with ideal conditions and/or estuarine species tolerance of low DO / low pH conditions (Weinstein, 2008). Further, in situ studies are needed to understand the effects of hypoxia and acidification in an ecosystem setting and to guide future management decisions.

Declaration of competing interest

The authors declare that they have no known competing financial interests or personal relationships that could have appeared to influence the work reported in this paper.

Acknowledgments

Funding for this study was obtained from the New York Sea Grant (award # R-FMB-38), the Laurie Landeau Foundation, and the Simons Foundation.

Appendix A. Supplementary data

Supplementary data to this article can be found online at https://doi.org/10.1016/j.marpolbul.2021.112908.

References

Aller, R.C., 1990. Bioturbation and manganese cycling in hemipelagic sediments. Philos. Trans. R. Soc. Lond. A 331, 51–68.

Barnes, R.T., Raymond, P.A., 2009. The contribution of agricultural and urban activities to inorganic carbon fluxes within temperate watersheds. Chem. Geol. 266, 318–327.

Barton, A., Hales, B., Waldbusser, G.G., Langdon, C., Feely, R.A., 2012. The Pacific oyster, Crassostrea gigas, shows negative correlation to naturally elevated carbon dioxide levels: implications for near-term ocean acidification effects. Limnol. Oceanogr. 57, 698–710.

Bauer, J.E., Cai, W.-J., Raymond, P.A., Bianchi, T.S., Hopkinson, C.S., Regnier, P.A.G., 2013. The changing carbon cycle of the coastal ocean. Nature 504, 61.

Baumann, H., Smith, E.M., 2018. In: Quantifying Metabolically Driven pH and Oxygen Fluctuations in US Nearshore Habitats at Diel to Interannual Time Scales, 41, pp. 1102–1117.

Baumann, H., Talmage, S.C., Gobler, C.J., 2012. Reduced early life growth and survival in a fish in direct response to increased carbon dioxide. Nat. Clim. Chang. 2, 38–41.

Baumann, H., Wallace, R., Tagliaferri, T., Gobler, C., 2015. Large natural pH, CO2 and O2 fluctuations in a temperate tidal salt marsh on diel, seasonal, and interannual time scales. Estuar. Coasts 38, 220–231.

Benotti, M.J., Abbene, M., Terracciano, S.A., 2007. Nitrogen Loading in Jamaica Bay, Long Island. Predevelopment to 2005. USGS, New York.

Breitburg, D., Levin, L.A., Oschlies, A., Grégoire, M., Chavez, F.P., Conley, D.J., Garçon, V., Gilbert, D., Gutiérrez, D., Isensee, K., Jacinto, G.S., Limburg, K.E., Montes, I., Naqvi, S.W.A., Pitcher, G.C., Rabalais, N.N., Roman, M.R., Rose, K.A., Seibel, B.A., Telszewski, M., Yasuhara, M., Zhang, J., 2018. Declining oxygen in the global ocean and coastal waters. Science 359.

Bruesewitz, D.A., Hoellein, T.J., Mooney, R.F., Gardner, W.S., Buskey, E.J., 2017. Wastewater influences nitrogen dynamics in a coastal catchment during a prolonged drought. Limnol. Oceanogr. 62, S239–S257.

Burnett, L.E., 1997. The challenges of living in hypoxic and hypercapnic aquatic environments. Integr. Comp. Biol. 37, 633–640.

Caffrey, J.M., 2004. Factors controlling net ecosystem metabolism in US estuaries. Estuaries 27, 90–101.

Cai, W.J., Hu, X.P., Huang, W.J., Murrell, M.C., Lehrter, J.C., Lohrenz, S.E., Chou, W.C., Zhai, W.D., Hollibaugh, J.T., Wang, Y.C., Zhao, P.S., Guo, X.H., Gundersen, K., Dai, M.H., Gong, G.C., 2011. Acidification of subsurface coastal waters enhanced by eutrophication. Nat. Geosci. 4, 766–770.

Cai, W.-J., Huang, W.-J., Luther, G.W., Pierrot, D., Li, M., Testa, J., Xue, M., Joesoef, A., Mann, R., Brodeur, J., Xu, Y.-Y., Chen, B., Hussain, N., Waldbusser, G.G., Cornwell, J., Kemp, W.M., 2017. Redox reactions and weak buffering capacity lead to acidification in the Chesapeake Bay. Nat. Commun. 8, 369.

Chen, M., Canelli, E., Fuhs, G.W., 1975. Effects of salinity on nitrification in the East River. J. Water Pollut. Control Fed. 47, 2474–2481.

Clark, H.R., Gobler, C.J., 2016. Diurnal fluctuations in CO2 and dissolved oxygen concentrations do not provide a refuge from hypoxia and acidification for early-life-stage bivalves. Mar. Ecol. Prog. Ser. 558, 1–14.

Codiga, D., Stoffel, H., Deacutis, C., Kiernan, S., Oviatt, C., 2009. Narragansett Bay hypoxic event characteristics based on fixed-site monitoring network time series: intermittency, geographic distribution, spatial synchronicity, and interannual variability. Estuar. Coasts 32, 621–641.

Connolly, T.P., Hickey, B.M., Geier, S.L., Cochlan, W.P., 2010. Processes influencing seasonal hypoxia in the northern California current system. J. Geophys. Res. 115, C03021.

Cornwall, C.E., Hurd, C.L., 2016. Experimental design in ocean acidification research: problems and solutions. ICES J. Mar. Sci. 73, 572–581.

Cotovicz, L.C., Knoppers, B.A., Brandini, N., Poirier, D., Costa Santos, S.J., Abril, G., 2018. Aragonite saturation state in a tropical coastal embayment dominated by phytoplankton blooms (Guanabara Bay – Brazil). Mar. Pollut. Bull. 129, 729–739.

Cyronak, T., Andersson, A.J., D'Angelo, S., Bresnahan, P., Davidson, C., Griffin, A., Kindeberg, T., Pennise, J., Takeshita, Y., White, M.J.E., Coasts, 2018. In: Short-Term Spatial and Temporal Carbonate Chemistry Variability in Two Contrasting Seagrass Meadows: Implications for pH Buffering Capacities, 41, pp. 1282–1296.

DePasquale, E., Baumann, H., Gobler, C.J., 2015. Vulnerability of early life stage Northwest Atlantic forage fish to ocean acidification and low oxygen. Mar. Ecol. Prog. Ser. 523, 145–156.

Diaz, R.J., 2001. Overview of hypoxia around the world. J. Environ. Qual. 30, 275–281.

Doney, S.C., Mahowald, N., Lima, I., Feely, R.A., Mackenzie, F.T., Lamarque, J.-F., Rasch, P.J., 2007. Impact of anthropogenic atmospheric nitrogen and sulfur deposition on ocean acidification and the inorganic carbon system. Proc. Natl. Acad. Sci. 104, 14580–14585.

Doney, S.C., Ruckelshaus, M., Duffy, J.E., Barry, J.P., Chan, F., English, C.A., Galindo, H. M., Grebmeier, J.M., Hollowed, A.B., Knowlton, N., Polovina, J., Rabalais, N.N., Sydeman, W.J., Talley, L.D., 2012. Climate change impacts on marine ecosystems. Annu. Rev. Mar. Sci. 4, 11–37.

Elena García-Martín, E., Serret, P., Pérez-Lorenzo, M., 2011. Testing potential bias in marine plankton respiration rates by dark bottle incubations in the NW Iberian shelf: incubation time and bottle volume. Cont. Shelf Res. 31, 496–506.

Feely, R.A., Alin, S.R., Newton, J., Sabine, C.L., Warner, M., Devol, A., Krembs, C., Maloy, C., 2010. The combined effects of ocean acidification, mixing, and respiration on pH and carbonate saturation in an urbanized estuary. Estuar. Coast. Shelf Sci. 88, 442–449.

Feely, R.A., Okazaki, R.R., Cai, W.-J., Bednaršek, N., Alin, S.R., Byrne, R.H., Fassbender, A., 2018. The combined effects of acidification and hypoxia on pH and aragonite saturation in the coastal waters of the California current ecosystem and the northern Gulf of Mexico. Cont. Shelf Res. 152, 50–60.

Fiedler, B., Fietzek, P., Vieira, N., Silva, P., Bittig, H.C., Körtzinger, A., 2012. In situ CO2 and O2 measurements on a profiling float. J. Atmos. Ocean. Technol. 30, 112–126.

Fietzek, P., Fiedler, B., Steinhoff, T., Körtzinger, A., 2014. In situ quality assessment of a novel underwater pCO2 sensor based on membrane equilibration and NDIR spectrometry. J. Atmos. Ocean. Technol. 31, 181–196.

Fribance, D.B., O'Donnell, J., Houk, A., 2013. Residual circulation in western Long Island sound. J. Geophys. Res. Oceans 118, 4727–4745.

Frieder, C.A., Nam, S.H., Martz, T.R., Levin, L.A., 2012. High temporal and spatial variability of dissolved oxygen and pH in a nearshore California kelp forest. Biogeosciences 9, 3917–3930.

Gazeau, F., Parker, L.M., Comeau, S., Gattuso, J.P., O'Connor, W.A., Martin, S., Portner, H.O., Ross, P.M., 2013. Impacts of ocean acidification on marine shelled molluscs. Mar. Biol. 160, 2207–2245.

Gobler, C., DePasquale, E., Griffith, A., Baumann, H., 2014. Hypoxia and acidification have additive and synergistic negative effects on the growth, survival, and metamorphosis of early life stage bivalves. PLoS One 9.

Gobler, C.J., Baumann, H., 2016. Hypoxia and acidification in ocean ecosystems: coupled dynamics and effects on marine life. Biol. Lett. 12, 20150976.

Gobler, C.J., Buck, N.J., Sieracki, M.E., Sanudo-Wilhelmy, S.A., 2006. Nitrogen and silicon limitation of phytoplankton communities across an urban estuary: the East River-Long Island sound system. Estuar. Coast. Shelf Sci. 68, 127–138.

Gobler, C.J., Clark, H.R., Griffith, A.W., Lusty, M.W., 2017. Diurnal fluctuations in acidification and hypoxia reduce growth and survival of larval and Juvenile Bay scallops (Argopecten irradians) and hard clams (Mercenaria mercenaria). Front. Mar. Sci. 3.

Gobler, C.J., Young, C.S., Goleski, J., Stevens, A., Thickman, J., Wallace, R.B., Curran, P., Koch, F., Kang, Y., Lusty, M.W., Hattenrath-Lehmann, T.K., Langlois, K., Collier, J.L., 2019. Accidental ecosystem restoration? Assessing the estuary-wide impacts of a new ocean inlet created by hurricane Sandy. Estuar. Coast. Shelf Sci. 221, 132–146.

Gordon, A.L., Bell, R.E., Carbotte, S.M., Flood, R.D., Hartig, E.K., Kolker, A.S., Gornitz, V., Peteet, D.M., Lieberman, L., Houghton, R.W., Huber, B.A., Rubenstone, J.L., Takesue, R., Geen, A.V., Langdon, C., Sambrotto, R.N., 2001. Integrated reconnaissance of the physical and biogeochemical characteristics of Jamaica Bay. Unpublished Report, online. Columbia Academic Commons. Available at: https://academiccommons.columbia.edu/doi/10.7916/D82Z1DPM.

Grear, J.S., O'Leary, C.A., Nye, J.A., Tettelbach, S.T., Gobler, C.J., 2020. Effects of coastal acidification on North Atlantic bivalves: interpreting laboratory responses in the context of in situ populations. Mar. Ecol. Prog. Ser. 633, 89–104.

Green, M.A., Aller, R.C., Aller, J.Y., 1998. Influence of carbonate dissolution on survival of shell-bearing meiobenthos in nearshore sediments. Limnol. Oceanogr. 43, 18–28.

Gribov, A., Krivoruchko, K., 2011. Local polynomials for data detrending and interpolation in the presence of barriers. Stoch. Env. Res. Risk A. 25, 1057–1063.

Hattenrath-Lehmann, T.K., Smith, J.L., Wallace, R.B., Merlo, L.R., Koch, F., Mittelsdorf, H., Gobler, C.J., 2015. The effects of elevated CO2 on the growth and toxicity of field populations and cultures of the saxitoxin-producing dinoflagellate, A lexandrium fundyense. Limnol. Oceanogr. 60 (1), 198–214.

Hofmann, G.E., Smith, J.E., Johnson, K.S., Send, U., Levin, L.A., Micheli, F., Paytan, A., Price, N.N., Peterson, B., Takeshita, Y., Matson, P.G., Crook, E.D., Kroeker, K.J., Gambi, M.C., Rivest, E.B., Frieder, C.A., Yu, P.C., Martz, T.R., 2011. High-frequency dynamics of ocean pH: a multi-ecosystem comparison. PLoS One 6.

Howland, R.J.M., Tappin, A.D., Uncles, R.J., Plummer, D.H., Bloomer, N.J., 2000. Distributions and seasonal variability of pH and alkalinity in the Tweed Estuary, UK. Sci. Total Environ. 251–252, 125–138.

Kelly, R.P., Foley, M.M., Fisher, W.S., Feely, R.A., Halpern, B.S., Waldbusser, G.G., Caldwell, M.R., 2011. Mitigating local causes of ocean acidification with existing Laws. Science 332, 1036–1037.

Kemp, W.M., Boynton, W.R., 1980. Influence of biological and physical processes on dissolved oxygen dynamics in an estuarine system: implications for measurement of community metabolism. Estuar. Coast. Mar. Sci. 11, 407–431.

Kemp, W.M., Boynton, W.R., Adolf, J.E., Boesch, D.F., Boicourt, W.C., Brush, G., Cornwell, J.C., Fisher, T.R., Glibert, P.M., Hagy, J.D., Harding, L.W., Houde, E.D., Kimmel, D.G., Miller, W.D., Newell, R.I.E., Roman, M.R., Smith, E.M., Stevenson, J. C., 2005. Eutrophication of Chesapeake Bay: historical trends and ecological interactions. Mar. Ecol. Prog. Ser. 303, 1–29.

Kinney, E.L., Valiela, I., 2011. Nitrogen loading to Great South Bay: land use, sources, retention, and transport from land to bay. J. Coast. Res. 672–686.

Koch, F., Gobler, C.J., 2009. The effects of tidal export from salt marsh ditches on estuarine water quality and plankton communities. Estuar. Coasts 32, 261–275.

Krivoruchko, K., Gribov, A., 2004. Geostatistical interpolation and simulation in the presence of barriers. In: geoENV IV—Geostatistics for Environmental Applications. Springer, pp. 331–342.

Kroeker, K.J., Kordas, R.L., Crim, R.N., Singh, G.G., 2010. Meta-analysis reveals negative yet variable effects of ocean acidification on marine organisms. Ecol. Lett. 13, 1419–1434.

Kroeker, K.J., Kordas, R.L., Crim, R., Hendriks, I.E., Ramajo, L., Singh, G.S., Duarte, C.M., Gattuso, J.P., 2013. Impacts of ocean acidification on marine organisms: quantifying sensitivities and interaction with warming. Glob. Chang. Biol. 19, 1884–1896.

Laurent, A., Fennel, K., Ko, D.S., Lehrter, J., 2018. Climate change projected to exacerbate impacts of coastal eutrophication in the northern Gulf of Mexico. Journal of Geophysical Research: Oceans 123, 3408–3426.

Levin, L.A., Ekau, W., Gooday, A.J., Jorissen, F., Middelburg, J.J., Naqvi, S.W.A., Neira, C., Rabalais, N.N., Zhang, J., 2009. Effects of natural and human-induced hypoxia on coastal benthos. Biogeosciences 6, 2063–2098.

Levinton, J., Doall, M., 2019. Feeding access of eastern oysters to the winter-spring phytoplankton bloom: evidence from Jamaica Bay, New York. J. Shellfish Res. 38 (115–121), 117.

Li, Y., Meseck, S.L., Dixon, M.S., Wikfors, G.H., 2018. The East River tidal strait, New York City, New York, a high-nutrient, low-chlorophyll coastal system. Int. Aquat. Res 10, 65–77.
Long, W.C., Swiney, K.M., Harris, C., Page, H.N., Foy, R.J., 2013. Effects of ocean acidification on juvenile red king crab (Paralithodes camtschaticus) and Tanner crab (Chionoecetes bairdi) growth, condition, calcification, and survival. PLoS One 8, e60959.
Marsooli, R., Orton, P.M., Fitzpatrick, J., Smith, H., 2018. Residence time of a highly urbanized estuary: Jamaica Bay, New York. J. Mar. Sci. Eng. 6, 44.
McGlathery, K.J., SundbÅfAck, K., Anderson, I.C., 2007. Eutrophication in shallow coastal bays and lagoons: the role of plants in the coastal filter. Mar. Ecol. Prog. Ser. 348, 1–18.
McLaughlin, K., Nezlin, N.P., Howard, M.D.A., Beck, C.D.A., Kudela, R.M., Mengel, M.J., Robertson, G.L., 2017. Rapid nitrification of wastewater ammonium near coastal ocean outfalls, Southern California, USA. Estuar. Coast. Shelf Sci. 186, 263–275.
Millero, F.J., 2010. Carbonate constants for estuarine waters. Mar. Freshw. Res. 61, 139–142.
Morrell, B.K., Gobler, C.J., 2020. Negative effects of diurnal changes in acidification and hypoxia on early-life stage estuarine fishes. Diversity 12, 25.
Murrell, M.C., Caffrey, J.M., Marcovich, D.T., Beck, M.W., Jarvis, B.M., Hagy 3rd., J.D., 2018. Seasonal oxygen dynamics in a warm temperate estuary: effects of hydrologic variability on measurements of primary production, respiration, and net metabolism. Estuaries Coast 41, 690–707.
NYCDEP, 2004. In: New York City's Wastewater Treatment System, pp. 1–34.
O'Donnell, J., Dam, H.G., Bohlen, W.F., Fitzgerald, W., Gay, P.S., Houk, A.E., Cohen, D. C., Howard-Strobel, M.M., 2008. Intermittent ventilation in the hypoxic zone of western Long Island sound during the summer of 2004. J. Geophys. Res. Oceans 113, 13.
O'Donnell, J., Wilson, R., Lwiza, K., Whitney, M., Bohlen, W.F., Codiga, D., Fribance, D., Fake, T., Bowman, M., Varekamp, J., 2014. The physical oceanography of Long Island sound. In: Latimer, J.S., Tedesco, M.A., Swanson, R.L., Yarish, C., Stacey, P.E., Garza, C. (Eds.), Long Island Sound. Springer, New York, pp. 79–158.
O'Shea, M.L., Brosnan, T.M., 2000. Trends in indicators of eutrophication in Western Long Island sound and the Hudson-Raritan Estuary. Estuaries 23, 877–901.
Paerl, H.W., Hall, N.S., Peierls, B.L., Rossignol, K.L., 2014a. Evolving paradigms and challenges in estuarine and coastal eutrophication dynamics in a culturally and climatically stressed world. Estuar. Coasts 37, 243–258.
Paerl, H.W., Hall, N.S., Peierls, B.L., Rossignol, K.L., Joyner, A.R., 2014b. Hydrologic variability and its control of phytoplankton community structure and function in two shallow, coastal, lagoonal ecosystems: the neuse and New River estuaries, North Carolina, USA. Estuar. Coasts 37, 31–45.
Parker, C.A., O'Reilly, J.E., 1991. Oxygen depletion in Long Island sound: a historical perspective. Estuaries 14, 248–264.
Parsons, T.R., Maita, Y., Lalli, C.M., 2013. A Manual of Chemical and Biological Methods for Seawater Analysis. Elsevier.
Ramesh, K., Melzner, F., Griffith, A.W., Gobler, C.J., Rouger, C., Tasdemir, D., Nehrke, G., 2018. In vivo characterization of bivalve larval shells: a confocal raman microscopy study. J. R. Soc. Interface 15.
n/a Rheuban, J.E., Doney, S.C., McCorkle, D.C., Jakuba, R.W., 2019. Quantifying the effects of nutrient enrichment and freshwater mixing on coastal ocean acidification. J. Geophys. Res. Oceans 124 (12), 9085–9100.
Roegner, G.C., Needoba, J.A., Baptista, A.M., 2011. Coastal upwelling supplies oxygen-depleted water to the Columbia River estuary. PLoS One 6, e18672.
Rysgaard, S., Risgaard-Petersen, N., Niels Peter, S., Kim, J., Lars Peter, N., 1994. Oxygen regulation of nitrification and denitrification in sediments. Limnol. Oceanogr. 39, 1643–1652.
Rysgaard, S., Risgaard-Petersen, N., Sloth, N.P., 1996. Nitrification, denitrification, and nitrate ammonification in sediments of two coastal lagoons in Southern France. In: Caumette, P., Castel, J., Herbert, R. (Eds.), Coastal Lagoon Eutrophication and ANaerobic Processes (C.L.E.AN.). Developments in Hydrobiology, 117.
Schulz, K.G., Riebesell, U., 2013. Diurnal changes in seawater carbonate chemistry speciation at increasing atmospheric carbon dioxide. Mar. Biol. 160, 1889–1899.
Shadwick, E.H., Friedrichs, M.A.M., Najjar, R.G., De Meo, O.A., Friedman, J.R., Da, F., Reay, W.G., 2019. High-frequency CO2 system variability over the winter-to-spring transition in a coastal plain estuary. J. Geophys. Res. Oceans 124 (11), 7626–7642.
Shen, C., Testa, J.M., Li, M., Cai, W.-J., Waldbusser, G.G., Ni, W., Kemp, W.M., Cornwell, J., Chen, B., Brodeur, J., Su, J., 2019. Controls on carbonate system dynamics in a coastal plain estuary: a modeling study. J. Geophys. Res. Biogeosci. 124, 61–78.
Soetaert, K., Hofmann, A.F., Middelburg, J.J., Meysman, F.J.R., Greenwood, J., 2007. The effect of biogeochemical processes on pH. Mar. Chem. 105, 30–51.
Sunda, W.G., Cai, W.J., 2012. Eutrophication induced CO2-acidification of subsurface coastal waters: interactive effects of temperature, salinity, and atmospheric P-CO2. Environ. Sci. Technol. 46, 10651–10659.
Tait, L.W., Schiel, D.R., 2013. Impacts of temperature on primary productivity and respiration in naturally structured macroalgal assemblages. PLoS One 8, e74413.
Talmage, S.C., Gobler, C.J., 2010. Effects of past, present, and future ocean carbon dioxide concentrations on the growth and survival of larval shellfish. Proc. Natl. Acad. Sci. U. S. A. 107, 17246–17251.
Talmage, S.C., Gobler, C.J., 2011. Effects of elevated temperature and carbon dioxide on the growth and survival of larvae and juveniles of three species of Northwest Atlantic bivalves. PLoS One 6.
Tomasetti, S.J., Morrell, B.K., Merlo, L.R., Gobler, C.J., 2018. Individual and combined effects of low dissolved oxygen and low pH on survival of early stage larval blue crabs, Callinectes sapidus. PLoS One 13, e0208629.
Turner, R.E., Rabalais, N.N., 2003. Linking landscape and water quality in the Mississippi river basin for 200 years. Bioscience 53, 563–572.
Turner, R.E., Rabalais, N.N., Justic, D., Dortch, Q., 2003. Global patterns of dissolved N, P and Si in large Rivers. Biogeochemistry 64, 297–317.
Tyler, R.M., Brady, D.C., Targett, T.E., 2009. Temporal and spatial dynamics of diel-cycling hypoxia in estuarine tributaries. Estuar. Coasts 32, 123–145.
Waldbusser, G.G., Brunner, E.L., Haley, B.A., Hales, B., Langdon, C.J., Prahl, F.G., 2013. A developmental and energetic basis linking larval oyster shell formation to acidification sensitivity. Geophys. Res. Lett. 40, 2171–2176.
Waldbusser, G.G., Hales, B., Langdon, C.J., Haley, B.A., Schrader, P., Brunner, E.L., Gray, M.W., Miller, C.A., Gimenez, I., 2015. Saturation-state sensitivity of marine bivalve larvae to ocean acidification. Nat. Clim. Chang. 5, 273.
Wallace, R., Gobler, C., 2015. Factors controlling blooms of microalgae and macroalgae (Ulva rigida) in a eutrophic, urban estuary: Jamaica Bay, NY, USA. Estuar. Coasts 38, 519–533.
Wallace, R.B., Baumann, H., Grear, J.S., Aller, R.C., Gobler, C.J., 2014. Coastal Ocean acidification: the other eutrophication problem. Estuar. Coast. Shelf Sci. 148, 1–13.
Wallace, R.B., Peterson, B.J., Gobler, C.J., 2021. Contrasting the dynamics of dissolved oxygen, carbonate chemistry, and ecosystem metabolism among distinct coastal habitat types. Front. Mar. Sci.
Weinstein, M.P., 2008. Ecological restoration and estuarine management: placing people in the coastal landscape. J. Appl. Ecol. 45, 296–304.
Yates, K.K., Dufore, C., Smiley, N., Jackson, C., Halley, R.B., 2007. Diurnal variation of oxygen and carbonate system parameters in Tampa Bay and Florida Bay. Mar. Chem. 104, 110–124.